SKBF
KBS
TEKNISK RAPPORT
79-19

Diffusion in the rock matrix – An important factor in radionuclide retardation?

Ivars Neretnieks

Royal Institute of Technology May 1979

SVENSK KÄRNBRÄNSLEFÖRSÖRJNING AB / PROJEKT KÄRNBRÄNSLESÄKERHET

POSTADRESS: Kärnbränslesäkerhet, Box 5864, 102 48 Stockholm, Telefon 08-67 95 40

E R R A T A

Diffusion in the rock matrix —
an important factor in radionuclide migration ?

by Ivars Neretnieks

page	5	line 1:	$\Psi K_d \rho_p / \varepsilon_f \ll 1$	should read:	$\Psi K_d \rho_p / \varepsilon_f \gg 1$	
"	10	" 5:	0.081	" "	0.095	
		" 13:	9.6 7.0	" "	7.7	5.3
		" 18:	1.25	" "	1.43	
"	17	eq. (17):	$\frac{D_p \varepsilon_p}{bU_f} < 1$	" "	$\frac{D_p \varepsilon_p}{bU_f} > 1$	
"	25	line 3 from bottom:	derivation	" "	differentiation	
"	26	last line in table:	$45 \cdot 10^9$	" "	$4.5 \cdot 10^9$	

IN/Esp

DIFFUSION IN THE ROCK MATRIX - AN IMPORTANT FACTOR IN RADIONUCLIDE RETARDATION?

Ivars Neretnieks
Royal Insititute of Technology May 1979

This report concerns a study which was conducted for the KBS project. The conclusions and viewpoints presented in the report are those of the author(s) and do not necessarily coincide with those of the client.

A list of other reports published in this series is attached at the end of this report. Information on KBS technical reports No. 1 - 120 in an earlier series is available through SKBF/KBS.

DIFFUSION IN THE ROCK MATRIX -

AN IMPORTANT FACTOR IN RADIONUCLIDE RETARDATION?

Address until
January 1980

Ivars Neretnieks
Earth Sciences Division
Lawrence Berkeley Laboratory
Berkeley, California 94720

Normal address

Department of Chemical Engineering
Royal Institute of Technology
S-100 44 Stockholm
Sweden

May 1979

TABLE OF CONTENTS

SUMMARY

Migration of radionuclides in the bedrock surrounding a repository is discussed. Available models use either a surface reaction or a bulk reaction concept to describe the retardation of migrating nuclides. The first model assumes that the nuclide reacts only with the surface of the fissures. This means that the rock matrix is not utilized. The other model implies that the whole bulk of the rock is accessible to the nuclides.

This paper analyses the accessiblity of the rock matrix to the radionuclides. The transport mechanisms are shown to be flow of water and nuclides in the fissures and transport of nuclides from the water in the fissures into the microfissures of the rock by diffusion. The diffusion of the nuclides into the rock and their sorption is the main retarding mechanism. The diffusivity of the nuclide is as important as its sorption equilibrium constant. Diffusivities in the pores and microfissures in such dense rocks as granite under confining pressure of hundreds of bars can be expected to be 6 - 20% of the diffusivity in water. These data are obtained from electrical resistivity measurements of salt water filled granites. Porosity of such granites varies from 0.4 - 0.9%. The apparent diffusivities in the granites will then vary between $0.25.10^{-12}/K_d\rho_p$ - $10.10^{-12}/K_d\rho_p$ m^2/s where $K_d\rho_p$ is the volume equilibrium constant. This varies from the porosity of the rock for nonsorbing species, to up to and over 10^4. For a 100 year contact time a nonsorbing nuclide can be expected to penetrate 10:s of meters of rock and a strongly sorbing nuclide with $K_d\rho_p$ larger than 10^4 will penetrate a few mm.

The diffusion into the rock matrix can enhance the retardation by many orders of magnitude as compared to retardation by surface reaction only. The retardation may on the other hand be many orders of magnitude smaller than if all the rock were accessible. This depends very much on the fissure widths and spacings.

A simple calculation shows that if a repository for spent fuel is surrounded by fissured but fairly good rock, ($K_p = 10^{-9}$ m/s and fissure spacing S = 50m) a thickness of 350 m will retard all radionuclides of importance until they have totally decayed except I-129, Cs-135 and U-238. Cs-135 will decay in another 1350 m of rock of the same quality.

DIFFUSION - AN IMPORTANT FACTOR IN RADIONUCLIDE RETARDATION

BACKGROUND

In the studies of disruptive events of final repositories for spent nuclear fuel (Campbell et al., Swedish KBS - study), leaching of the fuel by water and subsequent nuclide migration in the ground is always the major event from a consequences point of view. To determine the rate of nuclide migration, models describing water flow rates and paths, as well as nuclide migration rates have been designed.

All present models describing nuclide migration in the ground are based on an assumption that most of the radionuclides are retarded by some sorption mechanism. The sorption mechanisms are not well understood. Assumptions such as reversibility and instantaneous equilibration are therefore normally made.

To determine the retardation, laboratory measurements are performed where radionuclides are contacted with rock. These experiments are done over a time-span varying between days or weeks and up to many months. The uptake of radionuclide by the rock is measured. The so-measured radionuclide sorption capability of rock is used for calculating the expected retardation in the bedrock.

To use the laboratory measured uptake data for calculating migration in the bedrock, either of two assumptions on mechanisms are made. For porous bedrock where the water is assumed to flow evenly through all the pores, the bulk of the rock will be equilibrated with the nuclide containing water. This is called bulk reaction. For sparsely fissured bedrock the assumption

is that the flow is in the fissures the nuclide only reacts with the fissure surface. It does not penetrate to any appreciable depth into the rock matrix. This is called surface reaction.

In the first case - porous flow and bulk reaction, we may overestimate the retardation capacity of the rock, if in reality all parts are not accessed by the water. In the second case - fissure flow and surface reaction, we may considerably underestimate the retardation capacity of the bedrock if the radionuclides migrate into the rock. Microfissures and other pores in which diffusion can take place are known to exist in even dense crystalline rocks such as granite. The differences in these two retardation mechanism assumptions can be seen from the following.

For porous flow and bulk reaction the nuclide velocity in the bedrock can be determined by

$$U_i = \frac{U_{w,tot}}{1 + K_d \rho_s \frac{(1 - \varepsilon_{tot})}{\varepsilon_{tot}}} \qquad (1)$$

where U_i is the nuclide velocity, $U_{w,tot}$ is the water velocity in the pores, K_d is the bulk equilibrium constant, ε_{tot} is the porosity of the rock, and ρ_s is rock density (excluding pores). For the purpose of this paper, equation (1) is rewritten to be based on the velocity in the fissures $U_{w,f}$, as there are strong indications that most of the flow in crystalline rock occurs in fissures.

$$U_i = \frac{U_{w,f}}{1 + K_d \rho_p \frac{(1 - \varepsilon_f)}{\varepsilon_f}} \qquad (1b)$$

where $U_{w,f} = U_{w,tot} \cdot \varepsilon_{tot}/\varepsilon_f$, and ρ_p = rock density including pores.

For fissure flow and surface reaction,

$$U_i = \frac{U_{w,f}}{1 + K_a a \frac{(1 - \varepsilon_f)}{\varepsilon_f}} \qquad (2)$$

where $U_{w,f}$ is the water velocity in the fissures, K_a is surface equilibrium constant, and a is the fissure surface area per volume of rock. K_a or K_d may be determined from the same laboratory experiment; K_d by determining how much was sorbed by the mass of rock sample used and K_a by determining how much was sorbed per surface area of the sample.

The relation between K_a and K_d is

$$K_a = \frac{K_d \rho_p}{a} \qquad (3)$$

This relation is only formally correct as either (or both) K_a and K_d will depend on the particle size used in the experiment. The particle size determines the available surface per volume of rock - a.

If, in one experiment 1-mm spherical particles were used to determine the sorption, and in another experiment 0.1 mm particles were used, the latter particles have about 10 times larger outer surface per volume of paricles. The result would be two sets of K_d - K_a values where the ratio of K_a and K_d between the sets would differ by a factor 10.

In an attempt to use these data to determine the nuclide migration velocity in the bedrock, the use of equations (1) and (2) would give very confusing results. If the K_d values in the two experiments were equal - which means that both the 0.1 mm and the 1 mm particle reacted with a bulk reaction, the

K_a values would differ by a factor of 10. Equation (1) would give the same nuclide velocity based on both experiments. Equation (2) - assuming surface reaction - would give a 10 times larger migration velocity using the K_a-values from the small particle because the available surface in the bedrock a has a constant value independent of the sample size in the experiment. It is, however, not possible to conclude that the bulk reaction, equation (1), is applicable. The experiment proved only that the nuclide penetrated 1 mm particles. It might not penetrate the distances which must be considered in the actual bedrock, where the thickness of the rock may be many meters or 10's of meters.

A better way of describing the nuclide migration would be to use a utilization factor, Ψ. Ψ indicates the fraction of the rock which can be equilibrated with the water. In consolidated rock Ψ will depend, not only on available fissure surface, but also on the penetration thickness. The penetration thickness will depend on the contact time of radionuclide and bedrock.

To include this effect, equation (1b) should be written:

$$U_i = \frac{U_{w,f}}{1 + \Psi K_d \rho_p \frac{(1 - \varepsilon_f)}{\varepsilon_f}} \qquad (4)$$

Equation (4) describes the migration in a medium which is only partly (Ψ) accessible by the radionuclide. For fissured rock $\Psi = 2\bar{\eta}/S$, where $\bar{\eta}$ is the penetration thickness into the rock matrix and S is the fissure spacing. In figure 1 the penetration thickness is shown. It is strongly dependent on the contact time, as will be demonstrated later. Equation (4) is not suited for actual calculations but shows adequately why equations (1) and (2) are ill suited for calculating radionuclide migration. For retarding nuclides, where

$\Psi K_d \rho_p / \epsilon_f \gg 1$, the penetration thickness $\bar{\eta}$ is as important as the equilibrium constant itself.

The equilibrium constant K_d depends mostly on chemical and physical interaction phenomena. Some important factors in addition to those normally determining physical and chemical adsorption and ion exchange are given below.

- The rock may alter the transported species by reduction/oxidation (for example, the Fe(II) in granite may reduce U(VI) to U(IV) which is much less soluble).
- The rock, including the minerals, may be altered significantly over long times.
- The rock may supply anions to the water which may form complexes or precipitates with the species.

All these reactions may be very slow and are determined by the transport rate of some species in the rock matrix. The transport rate of the various species, including the radionuclides in the rock matrix, is a slow process as the transport is by diffusion in the small pores of the solid. Diffusion processes will thus be very important in determining the penetration thickness for the radionuclide.

If a homogeneous porous medium with an equilibrium constant K_d, is contacted with a fluid containing trace concentrations of a radionuclide, this will start diffusing into the medium. The depth of penetration may be determined by applying the equation of diffusion (Bird et al. 1960). For a stable species we have:

$$\frac{C}{C_o} = \operatorname{erfc} \frac{z}{2\sqrt{D_a t}} \tag{5}$$

Figure 2 shows the meaning of the penetration thickness (6). $\bar{\eta}$ is a fictitious distance in the body where the radionuclide sorbed was the equilibrium concen-

tration with the contacted liquid. The real concentration profile is depicted by curve I. The sorbed amount is proportional to the area under the curve. The area under curve II is the same as under I.

The penetration thickness $\bar{\eta}$ for this case can be obtained from the solution to the equation of diffusion:

$$\bar{\eta} = \frac{2}{\sqrt{\pi}}\sqrt{D_a t} \approx 1.13\sqrt{D_a t} \tag{6}$$

where t is the contact time and D_a is the apparent diffusivity in the rock matrix. The 1% concentration point $C/C_o = 0.01$ will reach about 4 times as far, $\eta_{0.01} = 4\sqrt{D_a t}$, (7a); and the 50% concentration point reaches $\eta_{0.5} = 0.95\sqrt{D_a t}$, (7b).

The apparent diffusivity D_a

The diffusion of a species in a porous body is normally slower than the diffusion in an unconfined fluid:

$$D_a = D_v \frac{\varepsilon_p \delta_D}{\tau^2 K_d \rho_p} = \frac{D_p \varepsilon_p}{K_d \rho_p} \tag{8}$$

δ_D is the constrictivity. It implies that the pores may be very constricted in some parts and thus seriously decrease the mobility of the species, τ is the tortuosity which accounts for the effect of a lengthening of the path, ε_p is the porosity which restricts the available mean area for transport and $K_d\rho_p$ is a volumetric sorption equilibrium constant.

$K_d\rho_p$ is equal to ε_p for a nonsorbing species, indicating that a nonsorbing species will be somewhat retarded by diffusing into the pores of the solid.

The diffusivity of a species of low molecular weight (M < 500) in water at ambient temperature is $D_v \approx 1\text{-}5 \cdot 10^{-9}$ m^2/s.

The constrictivity is very difficult to assess, but it is probably well below 1. Values for porous catalysts (Brakel 1974) indicate values down to 0.4. Tortuosity reduces the diffusivity by τ^2 = 2-3. The tortuosity and constrictivity are difficult to separate experimentally. The ratio of δ_D/τ^2 is usually determined. This ratio will be called the geometric factor in this paper. The sorption equilibrium factor $K_d\rho_p$ varies from very low values - ε_p for nonsorbing nuclides, to very large values 10^4 - 10^5 for strongly sorbing nuclides (Allard 1978) such as Americium.

Some observations regarding micro fissures in rocks

Most rocks, even dense crystalline rocks such as granite have been observed to be porous. Recently Brace (1977) measured cavity sizes and shapes for Westerly granite and Sherman granite by electron microscopy observations. Crack lengths varied from 0.075 to 250 μm and widths were between 0.01 and 10 μm for the Westerly granite. Sherman granite cracks were larger, 0.025-2500 μm long and 0.075-250 μm wide. Similar measurements were made by Hadley (1976). Brace (1977) discusses how the fissures change under stress and become less, or sometimes more accessible to flowing fluids. Brace et al. (1968) give data for permeability of granites. The permeability is strongly dependent on the confining pressure. At about 100 bar, a typical permeability of the granite matrix is 230 nd (nano darcy) which is equivalent to K_p about 2.10^{-12} m/s for water at ambient temperature. Such low permeabilities indicate that in practice all flow will take place in the fissures of the rock. A further indication of the accessibility of the micro fissures can be obtained from sorption measurements of gases. For a Swedish granite a BET - surface

12 m^2/g was observed (KBS 1977b) with nitrogen as sorbing gas. Erdal et al. (1979) measured BET surfaces - with nitrogen and with ethylene glycol for a climax stock granite from the Nevada test site. They found BET-nitrogen surfaces varying from 0.1 to 0.25 m^2/g. The surface increased with decreasing particle size. This increase can, however, not be explained by an increase of the outer surface of the particles. BET-ethylene glycol surfaces varied from 1.3 to 9 m^2/g and did not vary with particle size.

Potter (1978) made auto radiographs of granite samples injected with three different radionuclides, Na-22, Ni-63 and S-35. The results seem to indicate that most of the flow is along intergranular channels.

Experimental data on micro pore diffusivities in rock

Garrels et al. (1949) measured the diffusivity of KCl at 25-65° C through thin slabs of various limestones. The thickness was 1 to 2 mm. The cross sectional area was 1.67 cm^2. The experiments were performed by dividing two liquid filled compartments by the limestone wafer and measuring the amount of KCl transported through the wafer at steady state and for a known concentration difference. For 25° C two different limestones with porosities ε_p = 3.8 and 11.6% gave a $D_p/D_v = \delta_D/\tau^2 = 0.29$ which compares very well with data for other porous bodies (Perry p. 16-19). The data for the third limestone with ε_p = 36% gives δ_D/τ^2 = 0.29-0.7 for 25° C. For higher temperatures it was not possible to reconstruct the evaluated data.

Klinkenberg (1951) gives some literature data for sandstones and sand with porosities in the range 0.2 - 0.6 . There the geometric factor is δ_D/τ^2 = 0.25-0.7. He furthermore indicates that electrical conductivity and molecular

diffusion may depend in the same way on the geometric factor. This is substantiated by a measurement. This means that $\varepsilon_p \delta_D / \tau^2 = R_o / R_s$ where R_s is the resistivity of the water saturated granite sample and R_o is that of the salt water. Brace et al. (1965, 1968) have shown that for Westerley granite with porosity ranging from 0.001 to 1, the geometric factor, as determined by electrical resistivity measurement, is ε_p over the whole range of porosity. Microfissure surface conductivity influence was eliminated by using high conductivity salt solutions. The lowest porosities were obtained by compressing the granite with up to 10 000 bar effective confining pressure $\bar{P}$. Resistivity relative to water varied as $R_s/R_o = 130\sqrt{\bar{P}}\,(\bar{P}$ bar). Resistivities recalculated into geometric factors and total porosities are given for three different granites and a granodiorite in Table 1. The data are from Table 2 in Brace et al. (1965). In this pressure range (0-250 bar), the relation $\delta_D/\tau^2 = \varepsilon_p$ does not apply well and the data in Table 1 are used instead. In Figure 3, the geometric factor is plotted versus porosity ε_p and extrapolated to the porosity at zero confining pressure. For 100 bar confining pressure, which is roughly the vertical stress component for a water-saturated rock at 500 m depth, porosity varies betwen 0.4 and 0.6% and the geometric factor varies between 0.064 and 0.21.

Extrapolation to zero confining pressure give values of the geometric factor between 0.15-0.62. The granodiorite has considerably lower porosities and geometric factors over the whole range of confining pressure.

Table 1. Data on some rocks (Brace et al. 1965)

	Pressure Bars				
	50	100	250	500	0
Granite Casco					
δ_D/τ^2	0.12	0.081	0.063	0.039	0.15*
$\varepsilon_p \delta_D/\tau^2 \cdot 10^4$	5.8	4.0	2.0	1.0	
$\varepsilon_p \cdot 10^3$	4.9	4.4	3.2	2.7	6.5
Granite Stone Mountain					
δ_D/τ^2	0.27	0.21	0.13	0.083	0.62*
$\varepsilon_p \delta_D/\tau^2 \cdot 10^4$	12	8.3	4.3	2.3	
$\varepsilon_p \cdot 10^3$	4.4	4.0	3.4	2.8	5.5
Granite Westerly					
δ_D/τ^2	0.091	0.064	0.035	0.021	0.36*
$\varepsilon_p \delta_D/\tau^2 \cdot 10^4$	9.6	7.0	2.7	1.6	
$\varepsilon_p \cdot 10^3$	8.4	8.2	7.9	7.7	9.0
Granodiorite Cape Cod					
δ_D/τ^2	0.036	0.026	0.013	0.01	0.036
$\varepsilon_p \delta_D/\tau^2 \cdot 10^4$	1.25	1	0.48	0.34	
$\varepsilon_p \cdot 10^3$	4	3.8	3.6	3.4	4.0

* extrapolated values

Later work by Brace and Orange (1968) and Brace (1977) indicate that for granite which has been repeatedly stressed to near fracturing pressure, the induced fissures influence the resistivity in another way. The geometric factor is no longer proportional to ε_p for these fissures but becomes constant and was found to lie between 0.02-0.2 for 7 different rocks, including Westerley granite and a granodiorite.

Values of the geometric factor for granites would thus, with the at present very limited information available, be expected to be between 0.06 and 0.2 for 100 bar and 0.15-0.6 for 0 bar. Porosities are expected to be from 0.4-0.8% for 100 bar and only slightly larger, 0.5 - 0.9%, for 0 bar.

For granodiorite only Brace et al. (1965) and Brace et al. (1968), data on conductivity is available and indicates $\delta_D/\tau^2 = 0.026$ at 100 bars and 0.04 for 0 bar. Porosity ε_p is 0.38% and 0.4%, respectively. Duffy (1978 personal communcation Los Alamos) also measured porosity of granodiorite and found similar values; 0.2% and 0.36% at 100 bar respectively.

Norton and Knapp (1977) measured diffusivities in more than 60 rock samples 2-13 mm thick. The material ranged from fairly porous sedimentary rocks to dense metamorphic rocks. Total porosities ranged from 0.08-21%. It is not possible to separate porosity and geometric factor from these data. The product $\frac{\varepsilon_p \delta_D}{\tau^2}$ however ranges from $1.1\text{-}86 \cdot 10^{-4}$ with most values between $2 \cdot 10^{-4} - 10 \cdot 10^{-4}$. This is in very good agreement with the data shown in Table 1.

Assessment of the apparent diffusivity D_a

With the ranges for porosities ε_p , constrictivities δ_D, tortuousities τ, diffusivities D_v, and equilibrium constants $K_d\rho_p$, the apparent diffusivity D_a can be assessed from equation 8 for the migrating species.

In Table 2 below, expected D_a-ranges are shown for nonsorbing and some sorbing nuclides.

Table 2. Expected apparent diffusivities D_a m^2/s in granite for nonsorbing ($K_d\rho_p = \varepsilon_p$); weakly sorbing ($K_d\rho_p = 1$), intermediately sorbing ($K_d\rho_p = 100$), and strongly sorbing ($K_d\rho_p = 10^4$) nuclides.

	Low Value	High Value
$K_d\rho_p$		
ε_p = 0.004-0.009	0.6×10^{-10}	10×10^{-10}
1	0.24×10^{-12}	9×10^{-12}
100	0.24×10^{-14}	9×10^{-14}
10000	0.24×10^{-16}	9×10^{-16}

In the following examples the data in Table 3 will be used.

Table 3

$D_v = 2 \cdot 10^{-9}$ m^2/s
$\varepsilon_p = 0.005$
$\delta_D/\tau^2 = 0.1$

This gives:

$$D_p = D_v \cdot \delta_D/\tau^2 = 0.2 \cdot 10^{-9} \text{ m}^2/\text{s}$$

$$D_p\varepsilon_p = 10^{-12} \text{ m}^2/\text{s}$$

$$K_d\rho_p = \varepsilon_p,\ 1,\ 100,\ 10^4 \text{ m}^3/\text{m}^3$$

giving D_a values of $2 \cdot 10^{-10}$, 10^{-12}, 10^{-14}, and 10^{-16} m^2/s, respectively.

Penetration thickness $\bar{\eta}$

With equation 6 and the data in Table 3, the following penetration thicknesses $\bar{\eta}$ can be determined. These are shown in Table 4 for various times.

Table 4. Penetration thickness $\bar{\eta}$ mm

Time	1 day	1 week	1 month	1 year	100 years	10^4 years	10^6 years	10^8 years
nonsorbing $K_d\rho_p = \varepsilon_p$	4.2	11	23	79	790	7900	79000	790000
weakly sorbing $K_d\rho_p = 1$	0.29	0.78	1.6	5.6	56	560	5600	56000
Intermediately sorbing $K_d\rho_p = 100$	0.029	0.078	0.16	0.56	5.6	56	560	5600
Strongly sorbing $K_d\rho_p = 10^4$	0.0029	0.0078	0.016	0.056	0.56	5.6	56	560

Approximate values of the utilization factor ψ can be obtained if the fissure spacing is known $\psi = 2\eta/S$.

Breakthrough curves for flow in a fissure

When nuclides containing water flows in a fissure, the nuclide will migrate into the porous structure of the rock by diffusion. The water will thus be depleted of the nuclide. For very thick rock this can be described mathematically by the following expressions.

Diffusion in the rock is given by:

$$\frac{\partial C_p}{\partial t} = D_a \frac{\partial^2 C_p}{\partial z^2} - \lambda C_p \tag{9}$$

For flow and sorption from the water in the fissure we have:

$$\frac{\partial C_f}{\partial t} + U_f \frac{\partial C_f}{\partial x} = \frac{K_d \rho_p D_a}{b} \cdot \left.\frac{\partial C_p}{\partial z}\right|_{z=0} - \lambda C_f \tag{10}$$

C_p = concentration in water in pores

C_f = concentration in water in fissures

x = distance along fissure

z = distance into rock from fissure surface

b = half-width of fissure

U_f = water velocity in fissure

$K_d \rho_p$ = volumetric equilibrium constant.

λ = decay time constant.

For a system which is initially free of nuclide and where the nuclide concentration suddenly is increased to C_o at the inlet of the fissure ($x = 0$), the initial and boundary conditions are:

$$\text{IC} \qquad C_p = C_f = 0 \qquad t < t_o \text{ all } x \text{ and } z \tag{11}$$

$$\text{BC1} \qquad C_p = C_f = 0 \qquad \text{when } t > 0 \text{ for } z \to \infty \tag{12}$$

$$\text{BC2} \qquad \left\{ \begin{array}{ll} C_f = 0 & \text{for } t < t_o \\ C_f = C_o \cdot e^{-\lambda t} & \text{for } t_o \leq t \leq t_o + \Delta t \\ C_f = 0 & \text{for } t > t_o + \Delta t \end{array} \right\} \quad \text{at } x = 0 \tag{13}$$

For $\lambda > 0$, the solution is obtained by the Laplace transformation method. (For a stable species ($\lambda = 0$), for $t_o = 0$ and $\Delta t \to \infty$ the solution is available in the literature - Carslaw & Jaeger 2nd ed. p. 396).

$$\frac{C_p}{C_o} = e^{-\lambda t} \left\{ \operatorname{erfc}\left(\frac{G}{\sqrt{t - (t_w + t_o)}}\right) - \operatorname{erfc}\left(\frac{G}{\sqrt{t - (t_w + t_o + \Delta t)}}\right) \right\} \tag{14}$$

where $$G = \frac{D_p \varepsilon_p + \frac{1}{2} \frac{U_f (2b) z}{x}}{2b \sqrt{D_a}} \cdot t_w \tag{15}$$

The solution applies only for $t > t_w + t_o$ for the first erfc expression which otherwise is 0 and $t > t_w + t_o + \Delta t$ for the second erfc expression which otherwise is 0.

For the fluid in the fissures of the rock $\frac{C_f}{C_o}$ is obtained by setting $z = 0$. The boundary condition BC2, equation 13, is used here because it simulates a constant leach rate of a body containing a decaying nuclide. This is one of the important cases to study. Equations 14 and 15 apply only when the penetration thickness is considerably smaller than the fissure spacing. In the following t_o is set 0 and $\Delta t = \infty$.

Long time or slow velocity effect

The rock volume between two fissures eventually becomes equilibrated with the inflowing liquid. For a stable species the sorption starts to deviate from that described by equations (14) and (15) at about $t = 0.016\ S^2/D_a$*, where S is the fissure spacing (or slab thickness). Table 5 shows these times in years for some spacings and D_a values.

Table 5

D_a m^2/s	$2 \cdot 10^{-10}$	10^{-12}	10^{-14}	10^{-16}
$K_d \rho_p$	0.005	1	100	10 000
S				
2	10	2 000	200 000	20×10^6
50	6250	$1.3 \cdot 10^6$	$130 \cdot 10^6$	$13 \cdot 10^9$

For much longer times than these, the nuclide migration rate becomes constant and can be determined by equation 1 as the utilization factor ψ becomes 1.

Another slow velocity effect is the transport by diffusion only in the direction of flow. When flow is slow or when short distances are considered, transport by diffusion is quicker than by flow.

When the argument of equation 5 is smaller than that of equation 14, transport by diffusion in the flow direction is faster than transport by flow.

* the penetration depth $\eta_{0.01} \simeq S/2$ for this t.

This can be expressed, for

$$\frac{x}{2\sqrt{D_a t}} < \frac{D_p \varepsilon_p x}{2bU_f\sqrt{D_a (t - t_w)}} , \tag{16}$$

diffusion is faster.

When sorption effects are important compared to flow alone, i.e., $t >> t_w$, diffusion dominates over flow when

$$\frac{D_p \varepsilon_p}{bU_f} \gtrsim 1 \tag{17}$$

In the above comparison, it has been assumed that the diffusivity in x and z directions is equal, which may not be true for rock under nonequal stress.

The relation between the permeability, fissure spacing, concentration, and fissure width is not known in practice. Some assumptions must be made to get this relation; Snow (1968) used a model where fissures were assumed to be of equal width and to have equal spacing. The fissures have flat parallel walls. For this case, the relations are:

$$U_f = \frac{g}{12\nu} (2b)^2 i \tag{18}$$

$$K_p = \frac{g}{12\nu} (2b)^3 / S \tag{19}$$

where

g is the gravitational constant,

2b is the fissure width

i is the hydraulic gradient

K_p is the permeability

S is the fissure spacing

ν is the kinematic viscosity

For ambient temperature, $g/12\nu$ is about 10^6 m^2/s. The fissure width 2b(m) and fissure velocity U_f (m/s) are given in Table 5 for some different permeabilities K_p (m/s) and fissure spacings (m).

By applying equations 18 and 19, bU_f may be expressed in terms of K_p, S, and i. For ambient temperature we get $bU_f = 0.5iK_pS$ and thus :

$$D_p\varepsilon_p > 0.5iK_pS \qquad (20)$$

The smallest iK_pS used in the examples in this paper is $3 \cdot 10^{-12}$ m^2/s and thus $D_p\varepsilon_p$ must be greater than this value for pure diffusion to be the governing transport mechanism. This may thus be the case for good rock, $K_p < 10^{-9}$ m/s, and fairly narrow fissure spacing, 2m.

There is actually no need to determine U_f and b separately, if the spacings can be assessed and if we consider long times only ($t_w >> t$) and for $\bar{\eta} << S$. We note that $2bU_f/S = U_o$ is $m^3/m^2,s$ the flow rate in the rock.

This in practice is usually determined by a flow measurement using a higher than natural hydraulic gradient. U_o can thus be obtained directly by measurements of water flow rate and proportioning by the hydraulic gradient. This means that $2bU_f = K_p$. Fissure spacing is probably easier to measure than fissure width, which eliminates the need to use assumptions on the mechanisms of fluid flow in fissures. Equations (18) and (19) thus can be made superfluous for the calculations of transport times. They are useful, however, for getting insight in the flow mechanisms.

Table 6. Fissure width 2b(m) and velocity U_f (m/s) for various spacings -S(m) and permeabilities K_p (m/s).

K_p	10^{-5}		10^{-6}		10^{-7}		10^{-8}		10^{-9}	
S	2b	U_f	2b	U_f	2b	U_f	2b	U_f	2b	U_f
2	$2.7 \cdot 10^{-4}$	$2.2 \cdot 10^{-4}$	$1.3 \cdot 10^{-4}$	$4.8 \cdot 10^{-5}$	$5.9 \cdot 10^{-5}$	$1.0 \cdot 10^{-5}$	$2.7 \cdot 10^{-5}$	$2.2 \cdot 10^{-6}$	$1.3 \cdot 10^{-5}$	$4.8 \cdot 10^{-7}$
50	$7.9 \cdot 10^{-4}$	$1.9 \cdot 10^{-3}$	$3.7 \cdot 10^{-4}$	$4.1 \cdot 10^{-4}$	$1.7 \cdot 10^{-4}$	$8.8 \cdot 10^{-5}$	$7.9 \cdot 10^{-5}$	$1.9 \cdot 10^{-5}$	$3.7 \cdot 10^{-5}$	$4.1 \cdot 10^{-6}$

Analysis of the breakthrough curve of a stable species

From equation 14 it can be seen that sorption does not make itself felt when

$$\frac{D_a t_w (K_d \rho_p)^2}{(2b)^2} < 0.23 \qquad (21)$$

Then the time for the concentration $C_f/C_o = 0.5$ to arrive is less than 2 times that for pure plug flow without any adsorption. This means that for times

$$t < \frac{0.5(2b)^2}{D_a (K_d \rho_p)^2} \qquad (22)$$

the front travels essentially as a plug flow front with a velocity U_f. In a log-log diagram of $t_{0.5}$ versus x, the slope is 1 during a first period, thereafter the slope is 2, indicating that there is a very strong retardation which increases with time. Finally the slope again becomes 1 and the material behind the front becomes equilibrated. The first part will only be of interest for very large fissures and small contact times.

Figure 4 shows the breakthrough curves for a nonsorbing nuclide which may diffuse into the pores of the rock, for the case where 2b = 0.27 mm, $U_f = 2.2 \cdot 10^{-4}$ m/s ($K_p = 10^{-5}$ m/s, S = 2 m, i = 0.003 m/m), $\varepsilon_p = 0.005$, $D_p \varepsilon_p = 10^{-12}$ m^2/s.

The permeability given above indicates a very permeable rock such as can be found near the surface at depths less than 100 m. Even in rocks near the surface (depths < 50 m) Snow (1968) found practically no fractures larger than 0.25 mm. The data in the above example are therefore very large even for shallow rock.

It can be seen from the figure 4 that nonsorbing species do not travel with the "velocity of water." The "velocity of water" can be visualized as the velocity a particle would have, which does not have access to the pore volume of the rock. The water would bring a particle a distance of 1000 m in about 50 days whereas a nonsorbing solved species would build up to its half inlet concentration after 120 days. For a 10 km distance the particle would travel for 1.4 years in this fissure, whereas the solved species would reach $C_f/C_o = 0.5$ after 25 years.

The dashed part of the curves indicate that the diffusing component has penetrated more than half the fissure spacing (1 m) into the rock. The utilization factor $\psi = 1$. A diffusing species is then retarded by a factor $U_{w,f} = U_i = \varepsilon_p(1 - \varepsilon_f)/\varepsilon_f = 38$, as can be seen from equation 1b, with $K_d\rho_p = \varepsilon_p$ in this case. This factor will vary with fissure size and spacing, with water velocity and porosity of the rock matrix, and will attain its maximum value after different times depending on the other variables. From Fig. 4 and equation 14 it is seen that after a certain distance the curve form becomes constant. This means, among other things, that there always is a certain constant relation between the time of arrival of two concentrations, e.g., $C_f/C_o = 0.01$ and $C_f/C_o = 0.5$ - two arbitrarily chosen values. If the time for arrival of $C_f/C_o = 0.5$ is known, the time for any other relative concentration can then easily be calculated. This applies only for the fully developed profile and before the rock mass is fully penetrated. The last condition can be written $\bar{\eta} << S/2$.

Figures 5, 6, and 7 show the time $t_{0.5}$ for $C_f/C_o = 0.5$ to travel a given distance x. Parameters are the volume equilibrium constant, $K_d\rho_p$, which is varied from 0.005 ($= \varepsilon_p$) to 10^4. The hydraulic gradient has been chosen fairly low, 0.003 m/m. These curves can easily be constructed for any desired parameter value from $U_f = x/t_{0.5}$, "water velocity," for the short distances, equation 14 for intermediate distances and equation 1 for large distances. The crossovers from one part to another have been done manually in this case. This gives sufficient accuracy for the purposes of this paper.

Figure 5 has been constructed to give a basis for discussion of the odd fissure at large depths. In the Swedish permeability measurements at depths down to 500-600 m in granite (KBS 1977a), the general permeability in some instances was very low: $K_p \approx 10^{-9}$ m/s. Occasionally a streak of fissures with spacings not less than 30-50 m is found. This was interpreted as distinct fissure zones. Two packer permeability tests with packer spacing of 2 m give K_p:s $\approx 10^{-6}$ m/s. An example of a bore hole log from these studies is shown in Fig. 8 (KBS 1977a, p. 21). Obviously such fissure zones may occur even at fairly large depths. Such fissures will of course be avoided in a repository, but it can be instructive to consider such a fissure as an extreme case. The travel times for "water" are very short in such fissures, see figure 5. A species with $K_d\rho_p = 10^4$ m^3/m^3 will, however, be strongly retarded even in such a fissure. A particle would cover a distance of 1000 m in 0.7 years, a nondecaying solved species with the above $K_d\rho_p$ would need about 70,000,000 years to build up a $C_f/C_o = 0.5$ concentration. The nominal fissure width 2b is 0.13 mm in this case. This is larger than any fissure found by Snow (1968) at depths below 100 m.

Figure 6 is designed to show a case where there are fissures far apart: S = 50 m. The average permeability for the rock with these fissures is set to be 10^{-9} m/s. If the permeability of such a rock would be measured by a two packer test such as for Fig. 8, the permeability would be 0 for 48 m and $25 \cdot 10^{-9}$ m/s when the fissure is found. This means that the fissure is still fairly large for depths of 500 m.

In this case a particle would cover a distance of 1000 m in 7 years, a solved diffusing but nonsorbing species such as, e.g., iodide I^- or C-14 in carbonate, would "travel" for 30 000 years. A strongly sorbing nuclide such as Am^{3+} with $K_d\rho_p = 8 \cdot 10^4$ (Allard 1978), would travel about 1 m in one million years.

Figure 7 is constructed to examplify transport in "good rock." Such rock has been found in several boreholes in granite and gneiss in south Sweden (KBS 1979). An example of these measurements is given in Fig. 9. Permeability is constant $\sim 10^{-9}$ m/s as measured by two packer tests over 3 m distances. (Actually, one-packer tests, sealing of the hole below 300-350 m give average permeabilities over the underlying rock mass of less than 10^{-11} m/s) (KBS 1979b).

Figure 7 indicates that the utilization factor ψ is 1 for this type of rock. This means that for low flow rates and small fissure spacings the rock behaves like a porous body which is everywhere in contact and equilibrium with the flowing water.

A particle would, in this case, move 1000 m in 70 years, a nonsorbing species in 50 000 years, and a strongly sorbing nuclide ($K_d\rho_p = 10^4$)would have

traveled 50 m since the birth of the earth 5 billion years ago. In this case, the transport velocity by diffusion only is of the same magnitude as transport by flow.

Implication for a final repository of radioactive waste.

In order to get a simple measure whereby to judge if a travelling nuclide will reach the biosphere from the repository or not, the following simple rule is used. It is strictly applicable only to a nuclide originally present in the repository but can be modified to approximately apply to migrating daughter nuclides as well.

Rule: If the nuclide at no time reaches the "biosphere" with a concentration 10^{-9} times that in the repository, it has decayed.

Table 7 and Figure 10 show the most important radionuclides in a repository for spent fuel (KBS 1978) together with $K_d\rho_p$ values for granite, obtained by Allard (1978), on about 0.1 mm crushed material. Contact times in the K_d measurements were up to 7 months. Reducing conditions prevail in granite which contains Fe(II) (Jacks 1978, KBS 1978, KBS TR 90 1978).

The above criterion can be expressed in the number of half lives the nuclide must be underway on a given distance - the distance to the biosphere. By solving equation (14), for when it has a maximum value equal to 10^{-9}, we find that this will occur after about 14 half lives.

Then,

$$\lambda \left[\frac{D_a K_d \rho_p}{2b \left(\frac{U_f}{x} \right) \sqrt{D_a}} \right]^2 = 90 \; * \qquad (23)$$

For a value larger than 90 the concentration of the nuclide will never reach 10^{-9} C_o. This is shown in the fifth column in Table 7.

The decay chains which go through a series of nuclides are assessed by approximate calculations.

Member i + 1 is assumed to start its travel from the point where member i arrived at 14 half lives. This is the point beyond which the concentration of member i is less than 10^{-9} C_o. The distances which the daughters will travel are thus considerably smaller in reality.

It is seen from Tables 8 and 9 that the two important chains including Am-241, Np-237, Th-229 and Ra-226 will all decay well within a 350 m thick granite barrier of the quality assumed.

The only three nuclides which do not decay "totally" within 350 m are Cs-135, I-129, and U-238.

---

* This is obtained by derivation of equation 14 and equating 0, which gives the maximum point. Solving this simultaneously with equation (14) equal to 10^{-9}, gives the above results. It applies for $t >> t_w$.

Table 7. Most important radionuclides in a repository for spent fuel and their migration in granitic rock.

Nuclide	Initial Amount * per ton U Ci/ton	half life years	$K_d \rho_p$ ** m^3/m^3	Distance (m) in rock with $K_p=10^{-9}$ m/s S = 50 m i = 0.003 m/s for $C = C_o \cdot 10^{-9}$	Distance (m) for surface reaction*** $K_p = 10^{-9}$ S = 50 i = 0.003 m/s for $C = C_o \cdot 10^{-9}$
Cs-137	$1.1 \cdot 10^5$	30	170	4.1	1 400
Sr-90	$7.6 \cdot 10^4$	28	43	7.8	3 500
Am-241	$7.8 \cdot 10^2$a	458	86 000	0.7	130
Am-243	$2.1 \cdot 10^1$	7 370	86 000	2.9	2 300
Pu-239	$3.2 \cdot 10^2$	24 400	810	53	$0.8 \cdot 10^6$
Pu-240	$4.9 \cdot 10^2$	6 580	810	28	$0.2 \cdot 10^6$
Pu-241	$1.1 \cdot 10^5$	13.2	810	1.3	470
Pu-242	$1.4 \cdot 10^0$	379 000	810	210	$12 \cdot 10^6$
Cm-244	$2.0 \cdot 10^3$	17.6	43 000f	0.2	1 100
Tc-99	$1.4 \cdot 10^1$	210 000	135	380	$>10^7$
Np-237	$3.3 \cdot 10^{-1}$b	$2.1 \cdot 10^6$	3 240	250	$>10^7$
Cs-135	$2.5 \cdot 10^1$	$3 \cdot 10^6$	170	1 300	$>10^7$
I-129	$3.8 \cdot 10^2$	$17 \cdot 10^6$	0.005e	565 000	$>10^7$
Ra-226	$1.1 \cdot 10^0$c	1 600	1 350	10.6	6 400
Th-229	$8.5 \cdot 10^1$d	7 300	6 480	10.3	30 000
U-238		$45 \cdot 10^9$	3 240	36 200	$>10^7$

* Kjellbert 1977

** (Allard, Grundfelt KBS, 1978) reducing conditions.

***KBS used S = 1. This would reduce the distance by a factor of 50.

a builds up to $3.3 \cdot 10^0$ after 100 years from Pu-241

b builds up to $11 \cdot 10^0$ after 10^5 years from Am-241

c not initially there, builds up from Th-230, Max. conc. at 10^6 years

d not initially there, builds up from U-233, Max. conc. at 2×10^5 years

e $K_d \rho_p$ equal to porosity of granite matrix = 0.005

f assumed half than for Am

Table 8. The decay chain leading to Th-229 (Grundfelt 1978)

Nuclide	Half life years	Distance (m) beyond which $C < C_o \cdot 10^{-9}$
Cm-245	9 300	4.5
Pu-241	13.2	1.3
Am-241	458	0.7
Np-237	2.1×10^6	250
U-233	162 000	69
Th-229	7 300	10.3
	Total	336

Table 9. The decay chain leading to Ra-226. The chain via U-238 is ignored due to the very long half life of U-238: $4.5 \cdot 10^9$ years and the small amount coming from this chain (KBS 1978, Grundfelt).*

Nuclide	Half life years	Distance (m) beyond which $C < C_o \cdot 10^{-9}$
Am-242 H	152	0.4
Cm-242	0.5	0
Pu-238	86	3.2
U-234	247 000	85
Th-230	80 000	34
Ra-226	1 600	10.6
	Total	133

* Uranium will be practically immobilized in a reducing water because of its low solubility

Figures 11, 12, 13 and 14 show the breakthrough curves at various distances for the nuclides in Table 7. The figures apply to a case where every nuclide originates in the repository. No decay chains are accounted for.

Comparison with the surface reaction model

In the KBS report, 1978. the same equilibrium data were used but a surface reaction mechanism had to be used as no diffusion data could be firmly verified in the time available. A comparison with the surface reaction model can be directly made by the use of equation 4. The last column in Table 7 shows the distance traveled for this case. A comparison of the two last columns in Fig. 7 shows that if diffusion in the matrix is of the order of magnitude used in this paper we can expect to have a 10^3 - 10^4 times shorter travel distance than previously expected.

Implications on the measurement of sorption equilibrium

Sorption measurements of radionuclides are usually done on crushed material and the data are presented as K_d-values (ml/g). This indicates an underlying assumption that all the material in the particle has homogeneously reacted with the radionuclide and that an equilibrium has been reached. Some experimental data indicate that this may be the case; other data, however, seem to indicate that a surface reaction may be the relevant mechanism.

Rancon (1967) observed that carbonate rock particles sorbed Cs proportionally to the particle surface for large particles (diameter larger than 0.2 mm), but proportional to their mass for smaller particles. An experiment with a larger rock sample (surface area 25 cm) indicated that the sorption was time-dependent. The explanation offered by Rancon is that the Cs slowly diffuses

into the rock. Figure 15 shows some results from Rancon's sorption experiment. Seitz, et al., (1978) have made similar observations. They note that sorption is a bulk reaction for particles smaller than 0.5 mm.

Allard et al., (1978) measured sorption of Sr, Cs, and Am on granite surfaces with surface area 25 - 40 cm^2. Figs. 16, 17, and 18 show these results. They show a marked increase of K_d-values with time. Allard's (1978) K_d data on 14 radionuclides on fine granite particles (~ 0.1 mm) increased by a factor of 2 - 10 when contact time increased from a week to 6 - 7 months, which is a further indication of strong time dependence.

Seitz et al., (1978) measured sorption of Am by gray Hornblende Schist, using smooth surfaces 12.5 cm^2 large. Their data have been plotted as log relative concentration versus log square root of time in Fig. 19: $\log C/C_o = f(\log \sqrt{t})$. This is the type of plot which would be used to evaluate results from a batch experiment, when the sorption rate is determined by diffusion into the particles and when the sorption capacity of the solid is very large. In Fig. 20 the same plot has been used for Allard's data from Figs. 16, 17 and 18. It can be seen from these plots that equilibrium has not been reached and that the experimental points can be made to fit reasonably well to the theoretical curve. The theoretical curve is obtained by solving the diffusion equation for sorption in a flat slab (See appendix 1). Erdal et al., (1978) sorbed various radioncludes on crushed and sieved granite particles. Some of their results have been plotted on $\log C/C_o$ versus $(\log \sqrt{t})$ plots in Fig.21 and 22. This type of plot clearly indicates that equilibrium has not been reached even after over 60 days of contact time in particles as small as 0.1 to 0.15 mm.

The data in Figures 19 - 22 could be used for determining K_d-values if diffusivities were known. They are not known for the materials at hand and furthermore the crushed material has been severely stressed beyond its breaking point, which introduces new fissures (Brace 1977). In addition to this the crushed material has mostly been broken down to particle sizes which are smaller than the original crystal sizes of the granite. What this does to the sorption capacity and accessibility of sites is unknown at present.

Discussion

Many observations indicate that solved species will be able to diffuse into a water saturated rock matrix, even in such dense crystalline rocks as granite. The apparent pore diffusivity for nonsorbing species $D_p\varepsilon_p$ are expecpected to lie between $0.25 \cdot 10^{-12}$ - $10 \cdot 10^{-12}$ m^2/s for most small ions and molecules in granites. As water flow in granitic bedrock is expected to be in fissures which can be spaced fairly far apart, the diffusion into the rock matrix from the fissure will be the main retarding mechanism. For less dense rocks, this has been noted experimentally by Cathles et al., (1974). In a tracer experiment in the ground silica particles arrived quickly whereas diffusing sodium chloride salt did not arrive even after long time.

During the instationary phase when the host rock is not fully equilibrated, the influence of fissure width on transport velocity as well as on the transported quantity is very large. A fissure which is 2 times larger than another will transport $2^3 = 8$ times the quantity in the smaller fissure and the species will arrive $2^6 = 64$ times earlier than in the smaller fissure

(equations 14, 15). This indicates that the flow rates as well as the first arrival will be dominated by only a few of the largest flow channels.

The above retardation mechanism has some interesting implications on the measurement of "water" transport times, or "water ages" such as measured by e.g. the C-14. As an example, consider a case where Fig. 5 applies, which would be "typical" for surface (< 100 m deep) rocks. The measured transport time using C-14 over a 10 km distance would be 500 years (curve $K_d\rho_p = 0.005$). A colloid particle would, however, travel only for 5 years. For other fissure sizes other ratios of particle-to-solved species travel times are obtained. This of course raises the question: What do we mean by the age of a groundwater and how can a "water age" be used? Appendix 2 gives some more information on age dating.

This retarding mechanism, which is due to diffusion into the rock, may prove to be very important as was demonstrated by the example comparing retardation by a surface reaction mechanism and the matrix diffusion mechanism. Retardation factors many orders of magnitude larger can be expected if there is matrix diffusion.

Another important implication of the matrix diffusion is that the rock will play an important part in determining the chemical environment for the migrating species. This is specially important for such species which will change their charge or even turn from cationic to anionic forms. Allard (1978) demonstrated that Tc will sorb under reducing conditions when it is in the Tc (IV) state whereas it will be anionic in the Tc (VII) state. U, Pu and Np, three other important species, behave similarly. Furthermore, U (IV) is

very little soluble in reducing groundwaters (KBS 1978), Allard (1978) - a few microgram/ℓ. Pu and Np can also be expected to have low solubilities under reducing conditions.

For a rock which, like many granites, contains some reducing agents such as Fe (II), the four above nuclide species would be reduced to little soluble as well as strongly sorbing species as they migrate into the rock. This would apply even if they started in the oxidized state.

Conclusions

The possible diffusion into the rock matrix has very important implications on the transport of radionuclides from a final repository. If it can be proved beyond doubt that this mechanism is active and that the diffusivities are of the magnitude used here, then a few 100 m:s of good rock will be a most effective barrier for most of the radionuclides of importance in spent nuclear fuel.

The diffusivity must, however, be validated and not only for the times and distances which can be handled in a laboratory, but also by using geologic evidence for migration of ions.

It was demonstrated that the largest channels would have the dominating influence on the transport. Channel frequencies for the depths which may be used for repositories must therefore be better known.

REFERENCES

Allard, B., Kipatsi H, Torstenfelt, B. Adsorption of long lived radionuclides in clay and rock, Part 2. Chalmers University of Technology, April 1978. KBS Technical Report 98.

Bird, R.B., Stewart, W.E., Lightfoot, E.N., Transport phenomena. Wiley, 1960.

Brace, W.F., Permeability from resistivity and pore shape. J. Geophys. Res., 1977, 82, p. 3343.

Brace, W.F., Orange A.S., Electrical resistivity changes in saturated rocks during fracture and frictional sliding. J. Geophys. Res., 1968, 73, p. 1433.

Brace, W.F., Orange A.S., Madden. T.R. The effect of pressure on the electrical resistivity of water-saturated crystalline rocks. J. Geophys. Res., 1965, 70, p. 5669

Brace, W. F., Walsh, J. B., Frangos, W. T., Permeability of granite under high pressure, J. Geophys. Res., 1968, 73, p. 2225

van Brakel, J., Heertjes, P.M. Analysis of diffusion in macroporous media in terms of a porosity, a tortuosity and a constrictivity factor. Int. J. Heat Mass Transfer, 1974, 17, p. 1093

Campbell, J.E., Dillon, R. T., Tierney, M. S., Davis, H.T., McGrath, P.E., Pearson, F. J., Jr., Shaw, H. R., Helton, J. C., Donath, F. A., Risk methodology for geologic disposal of radioactive waste: Interim report. Sandia Laboratories, Albuquerque, New Mexico. Oct. 1978, NUREG/CR-0458, SAND78/0029 RW.

Carslaw, H.S., Jeager, J. C., Conduction of heat in solids, 1959, 2nd edition, Oxford University Press.

Cathles, L. M., Spedden, H. R., Malouf, E. E. A tracer technique to measure the diffusional accessibility of matrix bloc mineralization. Symposium , 103rd AIME annual meeting, Dallas 1974, p.129.

Crank, J., Mathematics of Diffusion, Oxford, 1956.

Duffy, C. J. Personal communication. Los Alamos Scientific Laboratories, University of California, 1978.

Erdal, B. R., Aguilar, R. D., Bayhurst, B. P., Daniels, W. R., Duffy, C. J., Lawrence, F. O., Maestas, S., Oliver, P. Q., Wolfsberg, K. Sorption-desorption studies on granite. I. Initial studies of Sr, Tc, Cs, Ba, Ce, Eu, U, Pu, Am. Los Alamos Scientific Laboratory, Feb. 1979, LA-7456-MS

Garrels, R. M., Dreyer, R. M., Howland, A. L., Diffusion of ions through intergranular spaces in water-saturated rocks. Geol. Soc. Am. Bull., 1949, 60, p. 1809.

Grundfelt, B., Nuclide migration from a rock repository for spent fuel. Kemakta konsult AB Stockholm Aug. 1978, KBS Technical Report No. 77.

Hadley, K. Comparison of calculated and observed crack densities and seismic velocities in westerly granite, J. Geophys. Res. 1976, 81, p. 3484

Jacks, G. Ground water chemistry at depth in granites and gneisses. Royal Institute of Technology, Stockholm Apr. 1978, KBS Technical Report No. 88

KBS Technical Report No. 90. Copper as an encapsulation material for unreprocessed nuclear waste - evaluation from the viewpoint of corrosion. Final report, March 1978. The Swedish Corrosion Research Institute and its reference group.

KBS-report. Handling of spent nuclear fuel and final storage of vitrified high-level reprocessing waste. Volume II, Geology. KBS, Stockholm, Nov. 1977a.

KBS-report. Handling of spent nuclear fuel and final storage of vitrified high-level reprocessing waste. Volume IV, Safety Analysis. KBS, Stockholm, Nov. 1977b.

KBS-report. Handling and final storage of unreprocessed spent nuclear fuel. Volume II. Technical. KBS, Stockholm, 1978.

KBS-report. Förglasat avfall från upparbetning. Kompletterande geologiska undersökningar KBS, Stockholm, Feb. 1979.

Kjellbert N. Emission rates in spent fuel and high-level waste from a PWR, calculated using ORIGEN. AB Atomenergi, April 1977,. KBS Technical Report No. 01.

Klinkenberg, L. J., Analolgy between diffusion and electrical conductivity in porous rocks. Geol. Soc. Am. Bull., 1951, 62, p. 559

Norton, D., Knapp, R., Transport phenomena in hydrothermal systems: The nature of porosity. Amer. J. Sci. 1977, 277, p. 913.

Perry, H., Chilton, C. H., Chemical engineers Handbook, 5th edition, McGraw-Hill, 1973

Potter, J. M. Eperimental permeability studies at elevated temperature and pressure of granite rocks. Los Alamos Scientific Laboratory, May 1978, Thesis,. LA-7224-T.

Rancon, D., Mechanisme de la contamination radioactive des roches consildees impermeable ou tres peu permeable. Disposal of radioactive wastes into the ground. Proceedings of a symposium, Vienna IAEA 1967, p. 179.

Seitz, M. G., Rickert, P. G., Fried, S. M., Friedman, A. M., Steindler, M. J. Transport properties of nuclear waste in geologic media. Draft annual report for the Waste Isolation Safety Assessment Program for the period Oct. 1, 1977 to Sept. 30, 1978. Argonne National Laboratory, 1978.

Snow, D. T. Rock fracture spacings, openings and porosities. J. Soil Mech. Found., Div., Amer. Soc. Civil. Eng., 1968, 94, (SM1), p. 73.

NOTATION

a	specific surface	m^2/m^3
b	half width of fissure	m
C	concentration in liquid	mol/m^3
C_f	concentration in liquid in fissure	mol/m^3
C_o	initial concentration in the liquid	mol/m^3
C_p	concentration in liquid in microfissure	mol/m^3
D_a	apparent diffusivity in solid	m^2/s
D_p	diffusivity in water in pores	m^2/s
D_v	diffusivity in water	m^2/s
g	gravitational constant	m/s^2
i	hydraulic gradient	m/m
K_a	surface equilibrium constant	m^3/m^2
K_d	equilibrium constant	m^3/kg
K_p	permeability	m/s
$\bar{P}$	confining pressure	bar
R_f	retardation factor	
R_o	resistivity of solution	ohm · m
R_s	resistivity of rock sample	ohm · m
S	fissure spacing	m
t	time	s, years
t_w	x/U_f water travel time	s, years
$t_{0.5}$	the time for the concentration to reach $C/C_o = 0.5$	s
U_f	velocity of water in a fissure - the velocity a non reacting particle would have	m/s

U_i	migration velocity of nuclide "i"	m/s
U_o	water flow rate	m^3/m^2, s
$U_{w,tot}$	U_o/ε_{tot} - average velocity in pores and fissures	m/s
$U_{w,f}$	velocity of water in fissures	m/s
x	distance along a fissure or in flow direction	m
z	distance into slab or body	m

ε_f	porosity of fissures
ε_{tot}	$\varepsilon_p + \varepsilon_t$ total porosity
ε_p	porosity of unfissured rock, matrix porosity
δ_D	constrictivity for diffusion
ρ_p	density of unfissured rock including pores kg/m^3
ρ_s	density of unfissured rock excluding pores kg/m^3
$\bar{\eta}$	penetration thickness m
$\eta_{0.01}$	penetration depth - the distance at which the concentration has risen to 1% of that at the surface m
τ	tortuosity
ν	kinematic viscosity m^2/s
ψ	utilization factor

APPENDIX 1

Application of the diffusion equation to batch sorption where the solid has a very large sorption capacity. The diffusion equation is:

$$\frac{\partial C_s}{\partial t} = D_a \frac{\partial^2 C_s}{\partial z^2},$$

where: C_s = concentration in the solid particle,
D_a = apparent diffusivity.

The concentration in the water C_1 in equillibrium with C_s is:

$$C_1 = C_s/K_d\rho;$$

The initial condition is:

$$C_1 = C_o; \quad C_s = 0 \text{ for } t \leq 0;$$

Boundary conditions are:

$$C_s = 0 \text{ for } z \rightarrow \infty$$

and $V_1C_1 = V_1C_o - V_s\bar{C}_s$,

where V_1 and V_s are liquid and solid volumes respectively.

The solution to this equation is (Crank, 1956),

$$\frac{C_1}{C_o} = e^{\theta} \operatorname{erfc}(\sqrt{\theta}) \quad \text{where}$$

$$\theta = \frac{D_a t}{\ell^2} \cdot \frac{V_s^2 \cdot (K_d \cdot \rho)^2}{V_1^2}$$

is a dimensionless time:

t = time

ℓ = thickness of sample contacted from one side.

For long times, θ, and when $\frac{V_1}{V_s K_d \rho} \ll 1$, the solution can be written:

$$\frac{C}{C_o} = \frac{1}{\sqrt{\pi}} \left(\frac{1}{\theta^{1/2}} + \frac{1}{2\theta^{3/2}} + \frac{1}{4\theta^{5/2}} \cdots \right)$$

APPENDIX 2

A note on age dating of groundwater by use of carbon 14

The carbonates in the water will diffuse into the matrix of the rock like the other species. At the inlet end the concentration is equal to that of fresh natural groundwaters $C = C_o$ at the fissure inlet.

Equations 9 and 10 may be used to describe the movement of C-14 carbonate in the rock matrix and the fissure respectively. The time dependent terms can be dropped as we have a stationary case. We then have

$$D_a \cdot \frac{\partial^2 C_p}{\partial z^2} = \lambda \; C_p \tag{1}$$

for the matrix and

$$u_f \frac{\partial C_f}{\partial x} = \frac{D_p \varepsilon_p}{b} \cdot \frac{\partial C_p}{\partial z}\bigg|_{z=0} - \lambda C_f \tag{2}$$

for the fissure.

The boundary conditions are

$$C_f = C_o \quad \text{at} \quad x = 0$$

$$C_p = C_f \quad \text{at} \quad z = 0 \quad \text{all } x$$

The solution to equations 1 and 2 are

$$\frac{C_f}{C_o} = e^{-\frac{x}{u_f}\left\{\frac{D_p \varepsilon_p}{b}\sqrt{\frac{\lambda}{D_a}} + \lambda\right\}} \tag{3}$$

The water "age" t_{C14} is determined from

$$-\lambda t_{C14} = \ln \frac{C_f}{C_o} \tag{4}$$

which when combined with equation 3 gives

$$t_{C14} = t_w \left(1 + \frac{2}{2b}\sqrt{\frac{D_p \varepsilon_p K_d \rho_p}{\lambda}}\right) \tag{5}$$

where t_w is the residence time of a particle which follows the water i.e. $t_w = x/u_f$ where u_f is the water velocity in the fissure.

Using the same data as in previous examples $K_p = 10^{-9}$ m/s, S = 50 m, i = 0.003 m/m and $K_d\rho_p = \varepsilon_p$ for a nonsorbing species we get

$$\frac{t_{C14}}{t_w} = 1950$$

In fairly low permeability rock $K_p = 10^{-9}$ m/s we thus will find water "ages" many thousand times larger than the time a particle would travel the same distance.

Typically for S = 50 m and a distance of 376 m the water age is one half life = 5730 years whereas the time for the water to move this distance is 2.9 years.

This to my opinion should make us consider what we mean by water age.

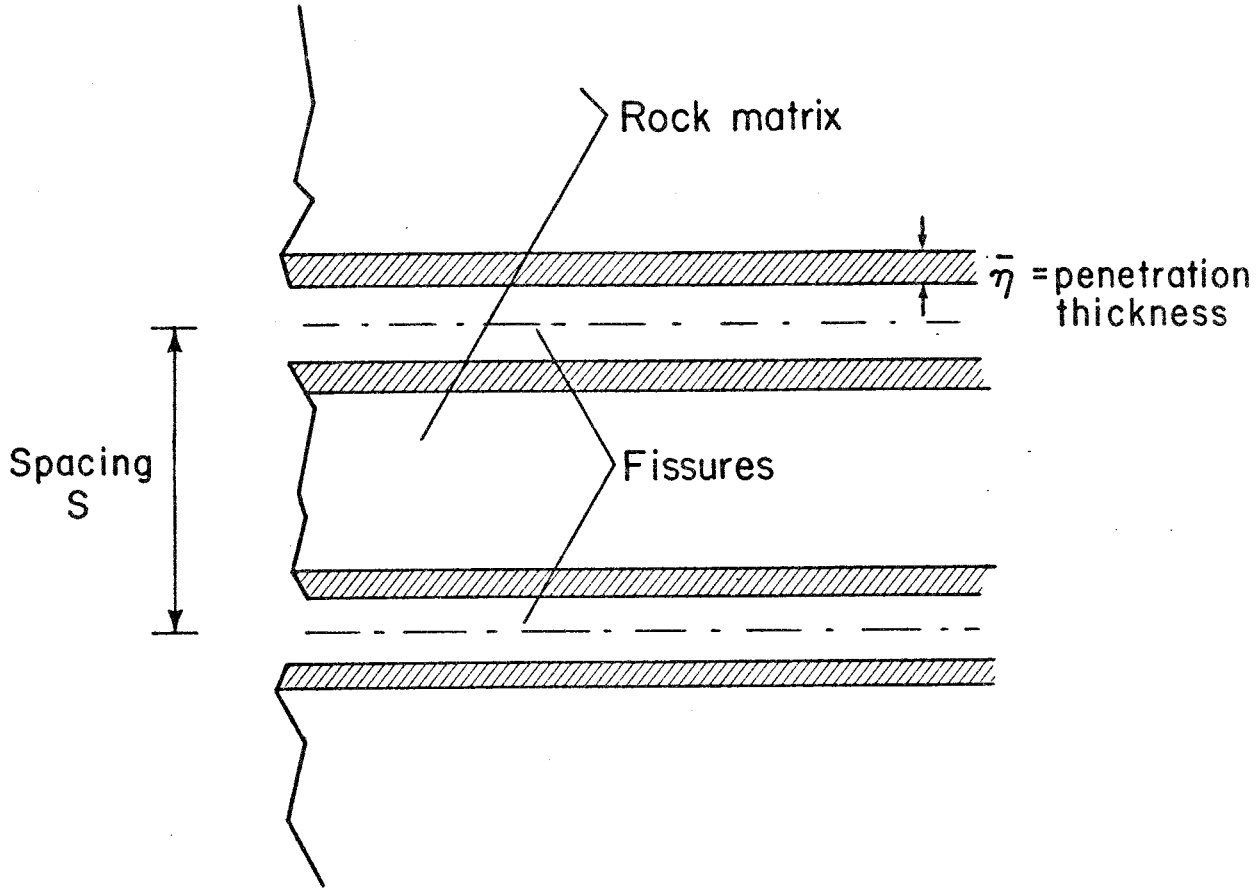

Figure 1 Fissure flow and sorption by diffusion into the rock matrix.

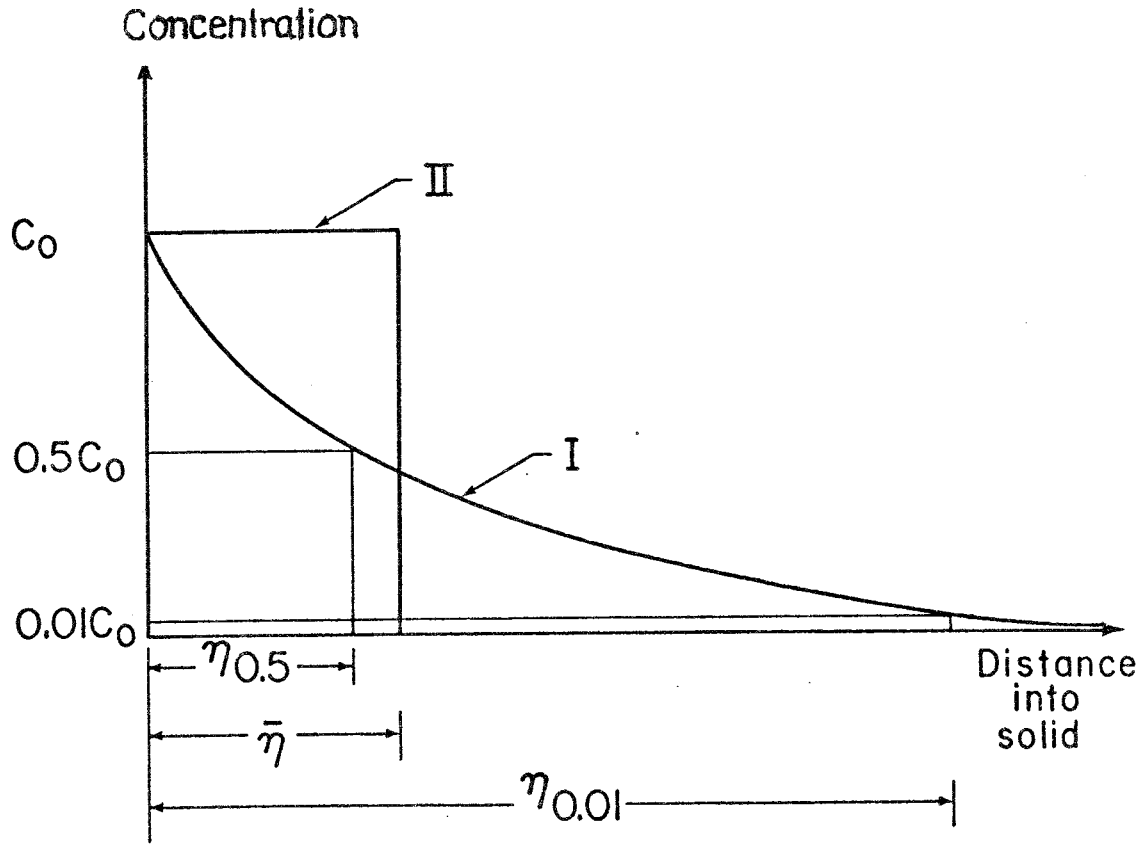

Figure 2 Penetration of a species into the rock matrix. Curve I: Concentration profile. Curve II: Shows penetration thickness $\bar{\eta}$.

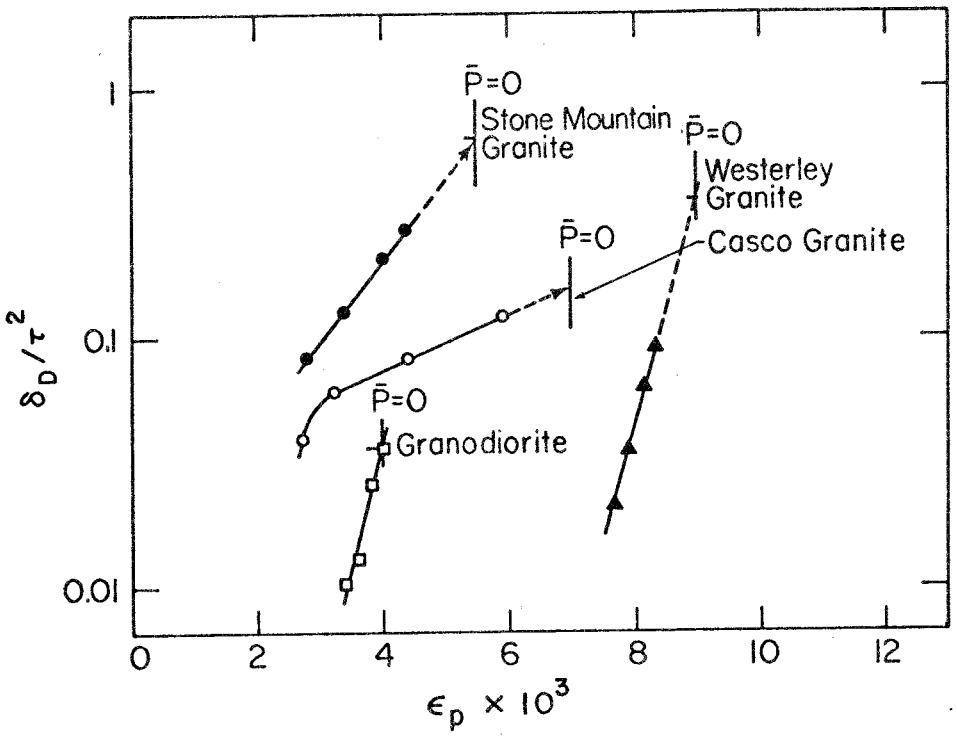

Figure 3 Geometric factor δ_D/τ^2 measured for various granites by Brace et al., (1965). The points from right to left are obtained for effective confining pressures 50, 100, 250, and 500 bar.

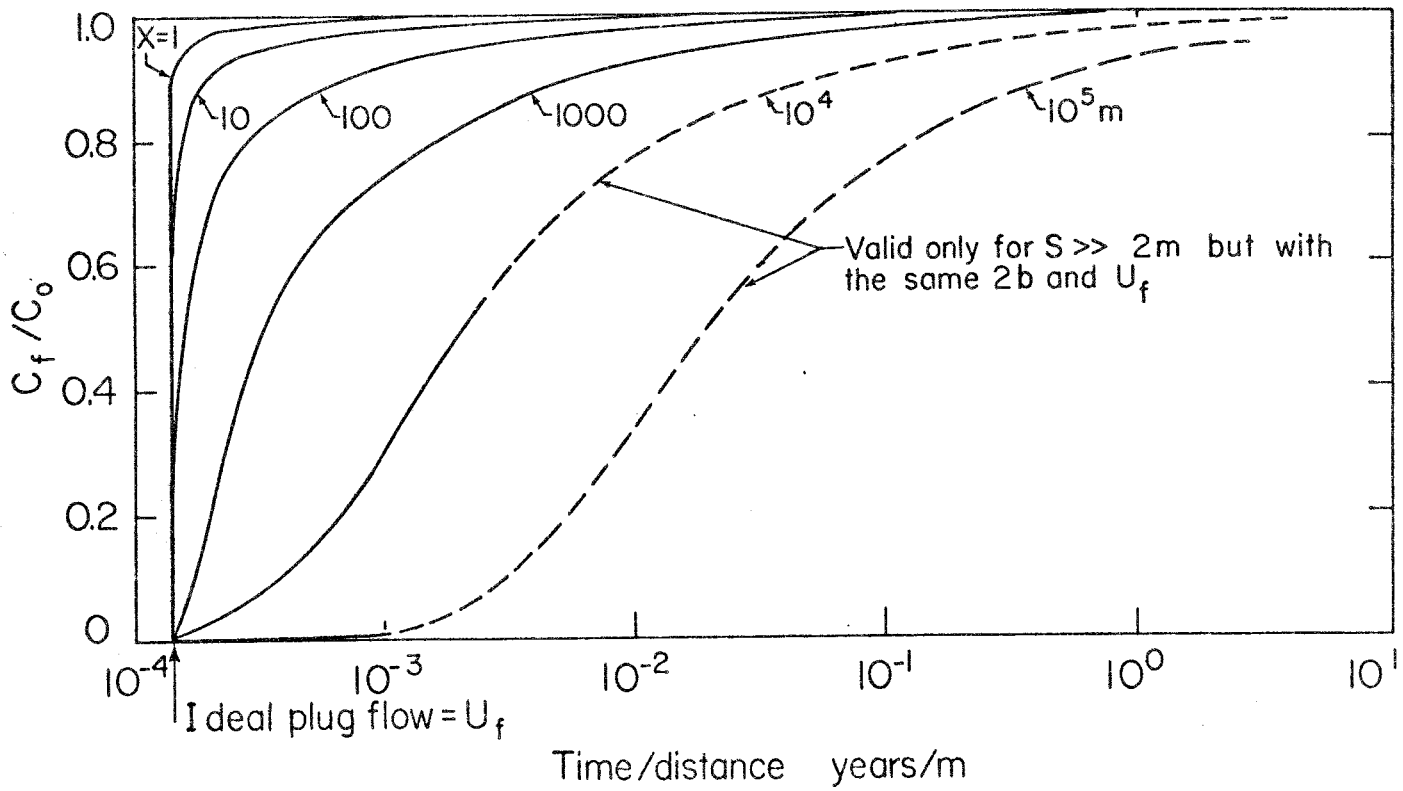

Figure 4 Breakthrough curves for a nonsorbing species which can diffuse into the pores of the matrix, $K_d\rho_p = 0.005$, $D_p\varepsilon_p = 10^{-12}$ m^2/s, $K_p = 10^{-5}$ m/s, i = 0.003 m/m, S = 2 m, $U_f = 2.2 \cdot 10^{-4}$ m/s, $2b = 2.7 \cdot 10^{-4}$ m.

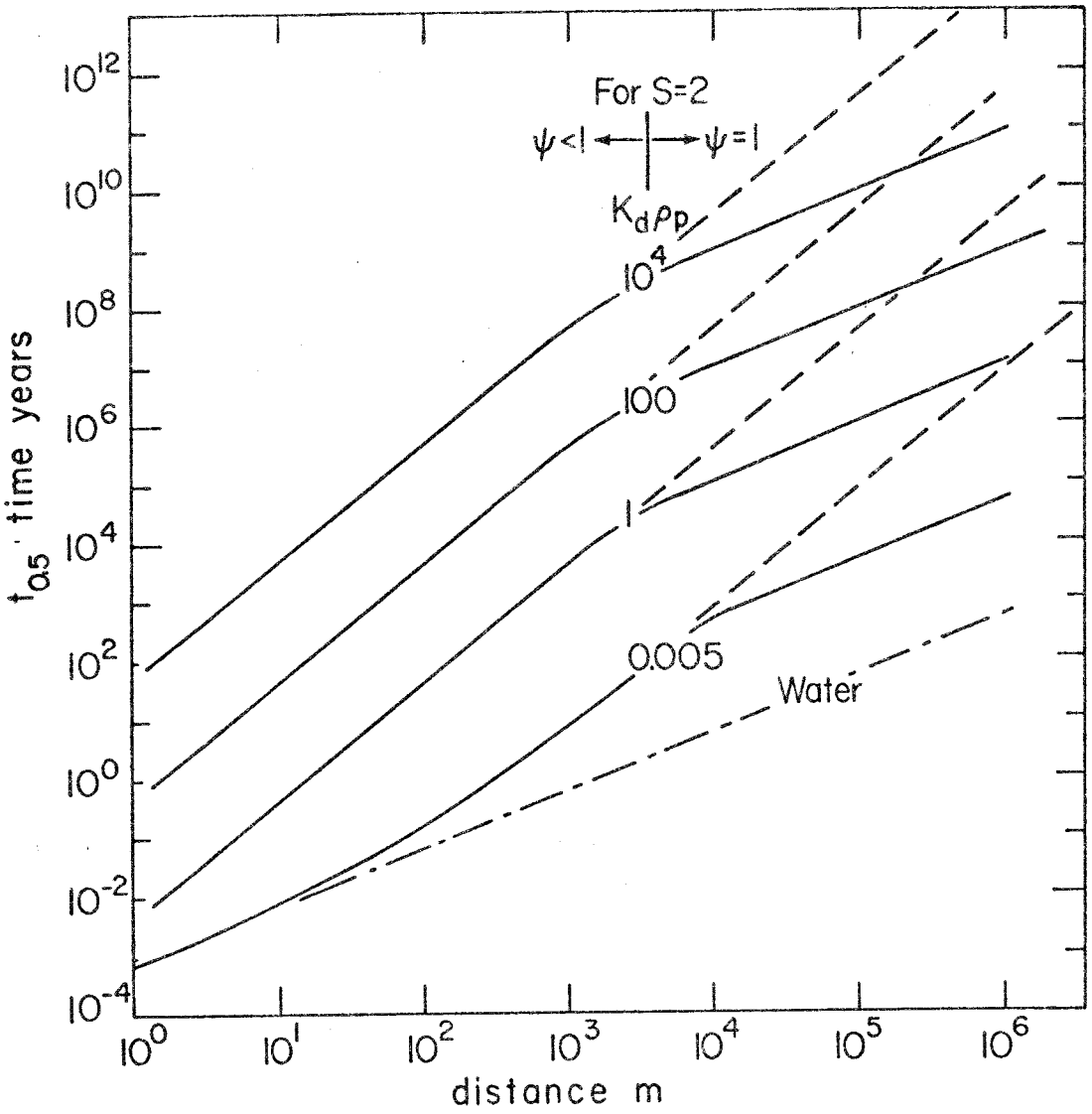

Figure 5 Time $t_{0.5}$ for the concentration $C/C_o = 0.5$ to travel a given distance. Dashed lines indicate that spacing is very large and that the rock between the fissures does not get fully penetrated. $K_p = 10^{-6}$ m/s, S = 2 m, i = 0.003 m/m, $D_p\varepsilon_p = 10^{-12}$ m^2/s, 2b = 0.126 mm, $U_f = 4.76 \cdot 10^{-5}$ m/s.

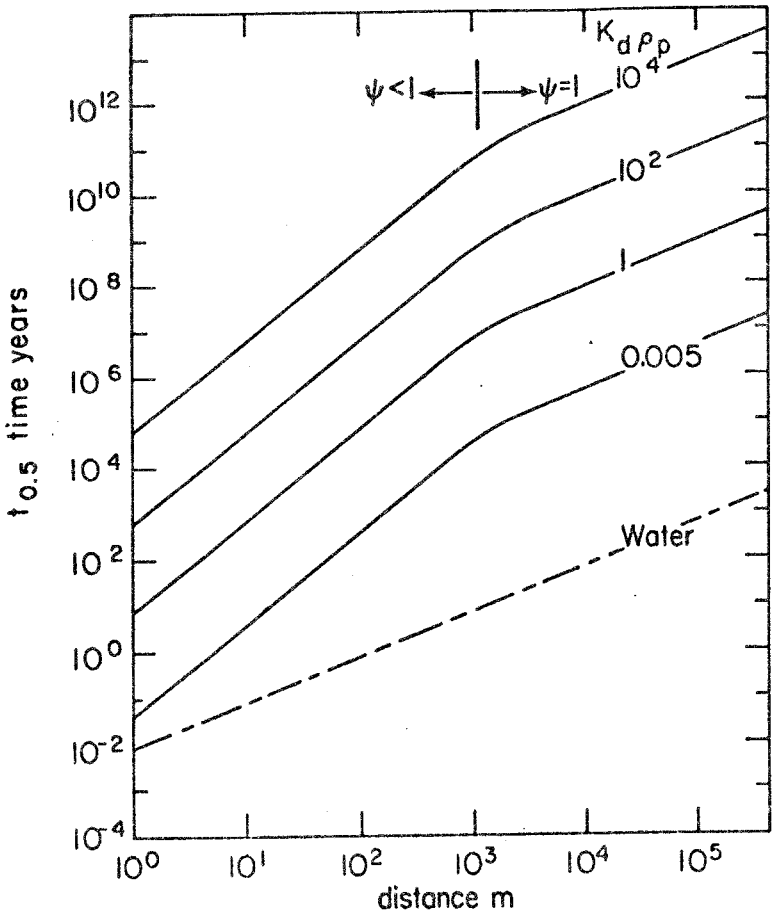

Figure 6 Time $t_{0.5}$ for the concentration $C/C_o = 0.5$ to travel a given distance. $K_p = 10^{-9}$ m/s, S = 50 m, i = 0.003 m/m, $D_p \varepsilon_p = 10^{-12}$ m^2/s, 2b = 0.037 mm, $U_f = 4.1 \cdot 10^{-6}$ m/s.

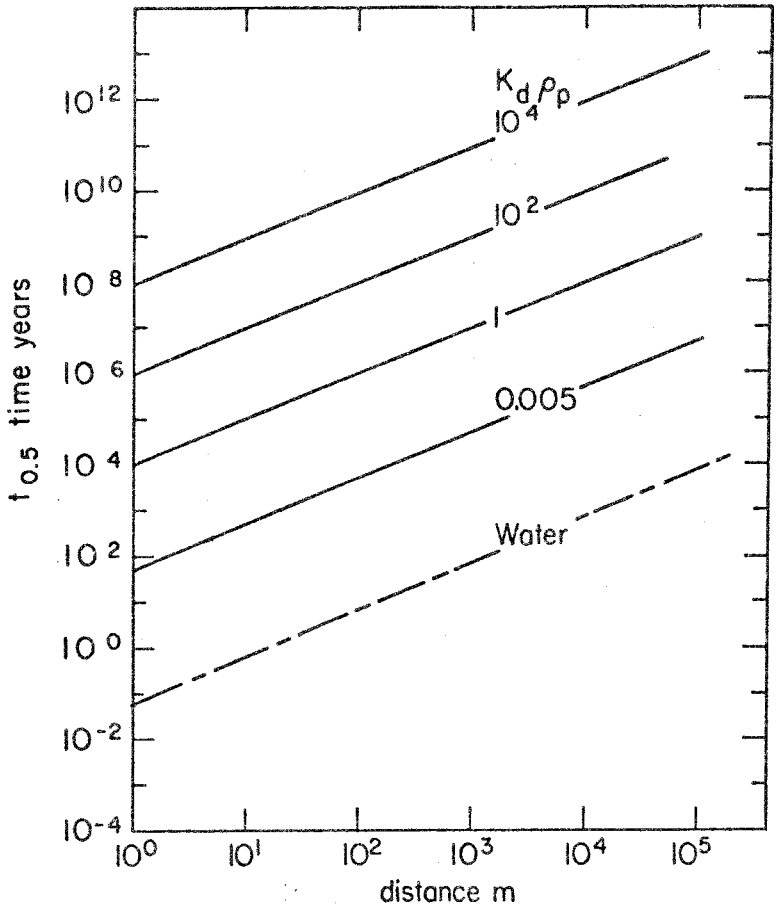

Figure 7 Time $t_{0.5}$ for the concentration $C/C_o = 0.5$ to travel a given distance. $K_p = 10^{-9}$ m/s, S = 2 m, i = 0.003 m/m, $D_p\varepsilon_p = 10^{-12}$ m/s, 2b = 0.013 mm, $U_f = 4.8 \cdot 10^{-7}$ m/s.

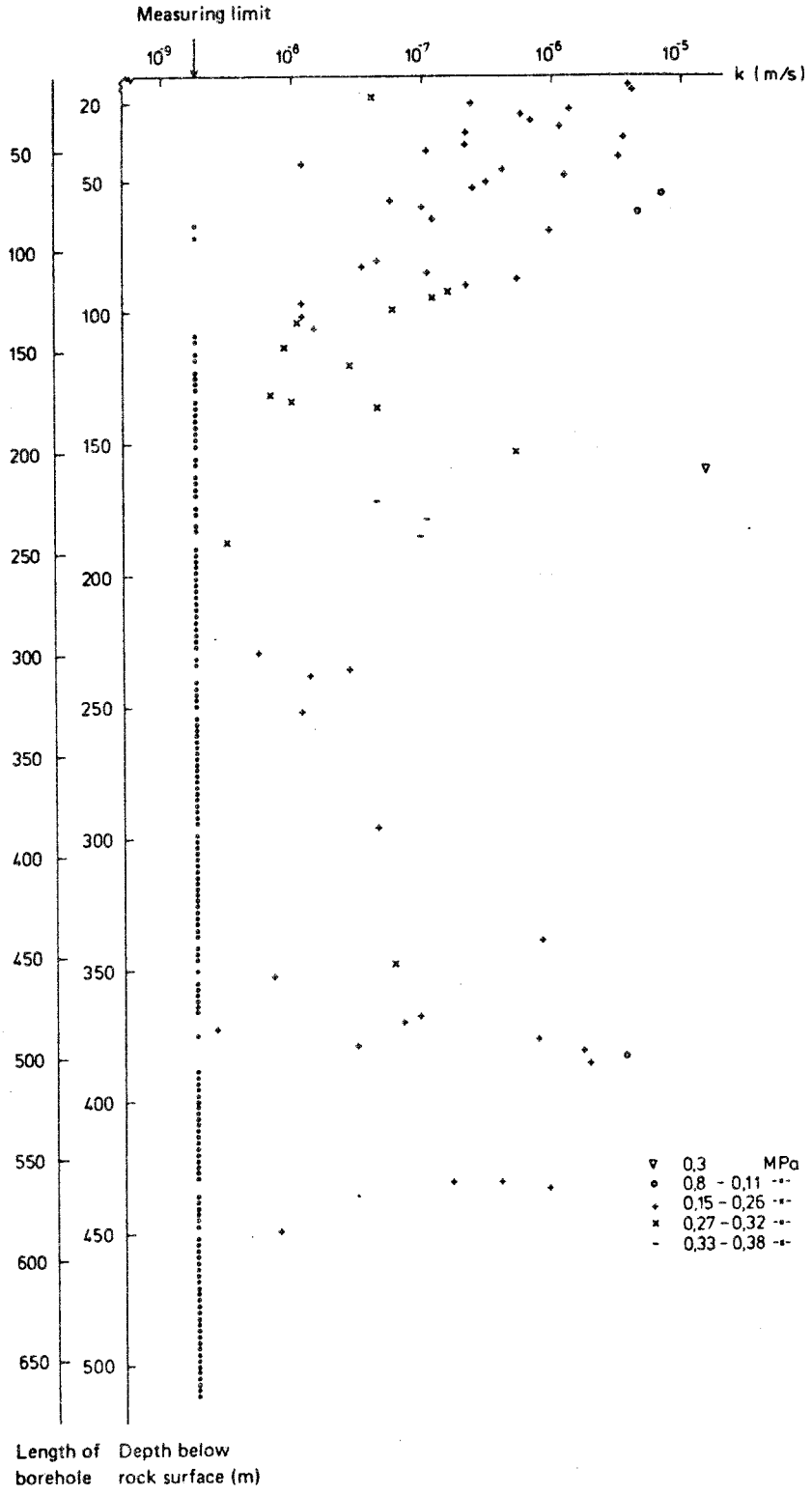

Figure 8 Permeability of hole 2 at Finnsjön (KBS-report, 1977a).

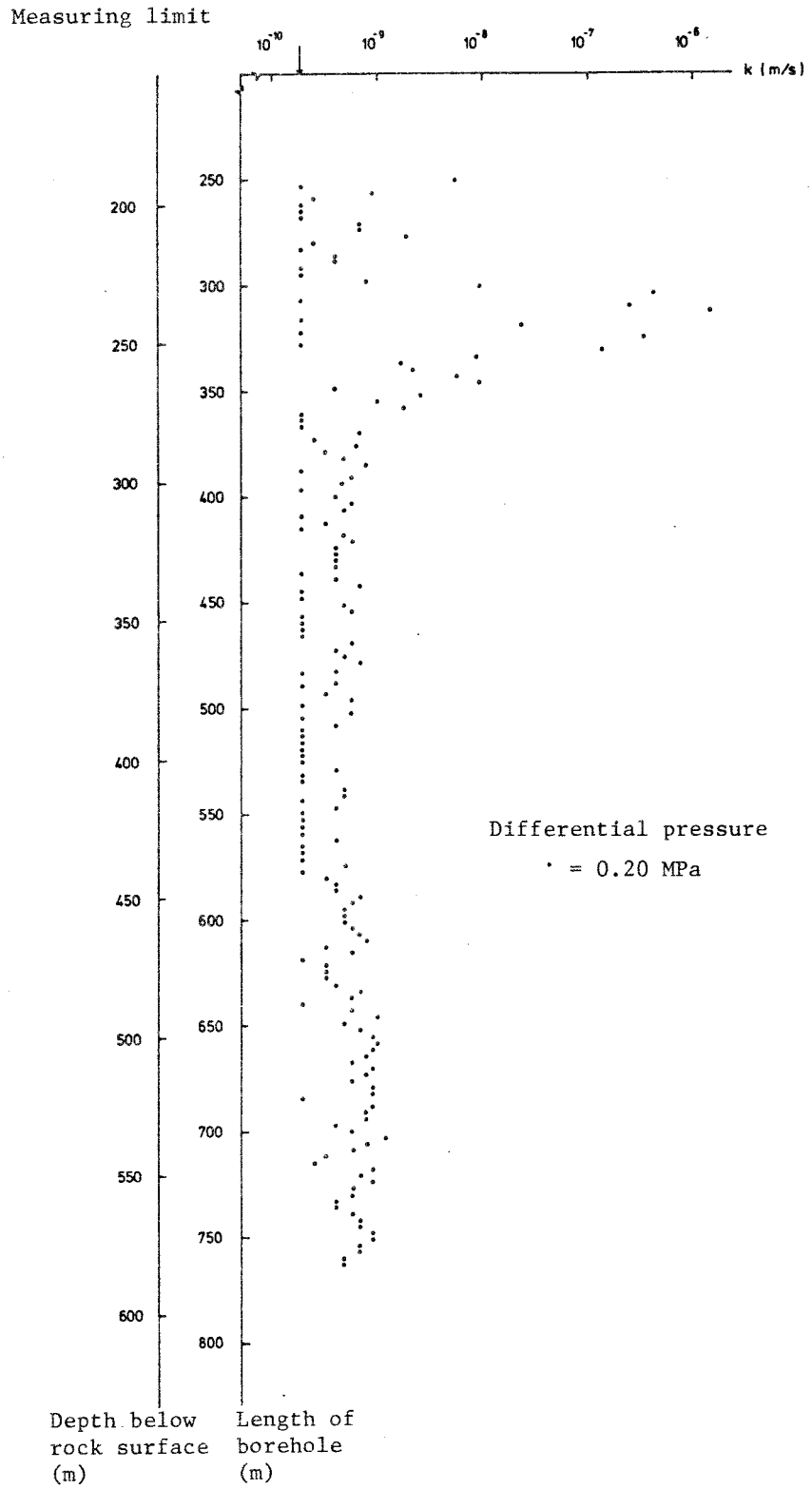

Figure 9 Permeability of hole Ka3 at Karlshamn (KBS-report, 1979).

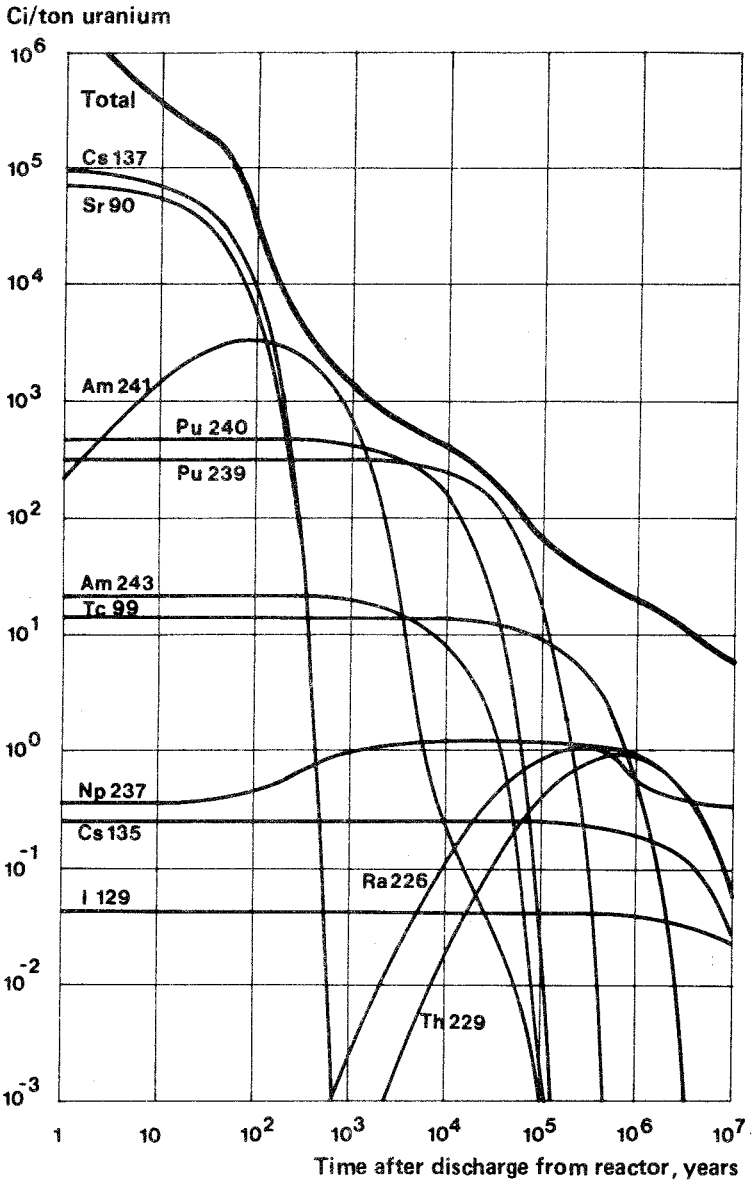

Figure 10 Radioactive elements in spent fuel. The graph shows the radioactive elements in PWR fuel with a burnup of 33,000 MWd(t)/tU, power density 34.4 MW(t)/tU and enrichment 3.1% uranium-235.

FIGURE 11

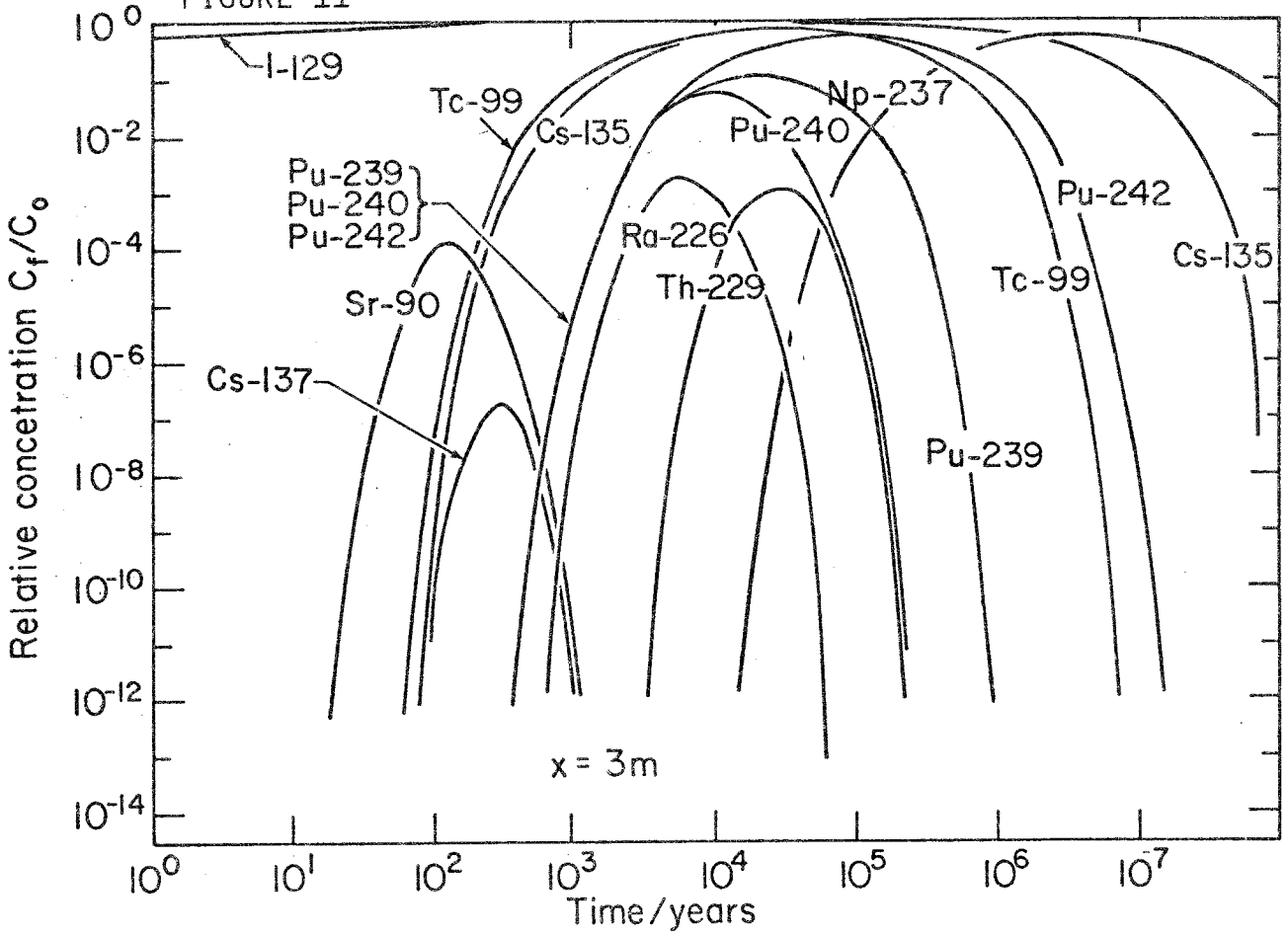

Figures 11-14 Breakthrough curves at distances 3, 10, 100 and 300 m for the 15 most important radionuclides in spent fuel. The case depicted applies for the nuclide originally present in the repository. $K_p = 10^{-9}$ m/s average over fissure spacing of 50 m, i = 0.003 m/m, $D_p \varepsilon_p = 10^{-12}$ m^2/s, 2b = 0.037 mm, $U_f = 4.1 \cdot 10^{-6}$ m/s.

FIGURE 12

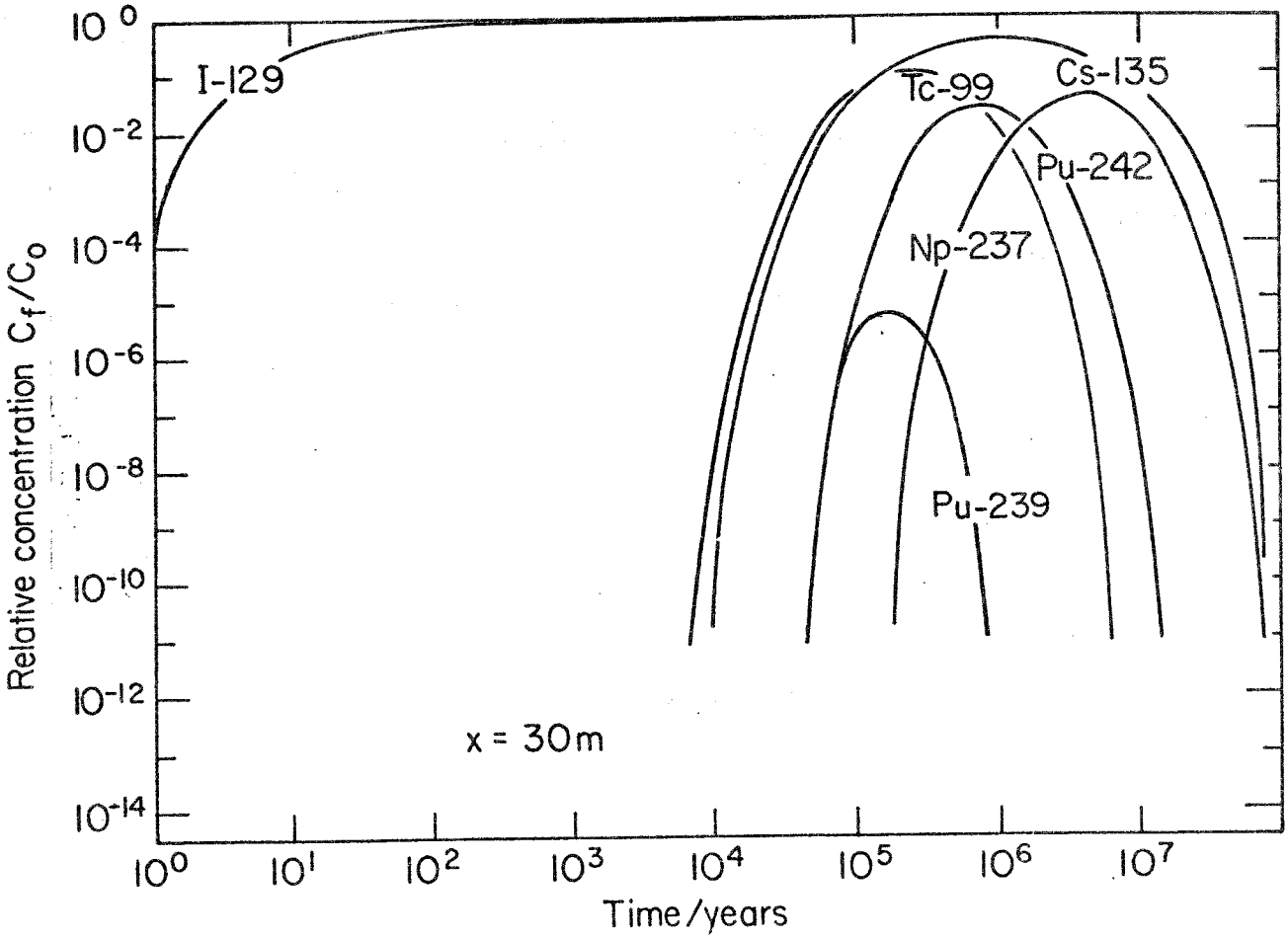
Relative concentration C_f/C_o
10^{0}
10^{-2}
10^{-4}
10^{-6}
10^{-8}
10^{-10}
10^{-12}
10^{-14}
I-129
Tc-99
Cs-135
Pu-242
Np-237
Pu-239
x = 30m
10^{0}
10^{1}
10^{2}
10^{3}
10^{4}
10^{5}
10^{6}
10^{7}
Time/years

FIGURE 13

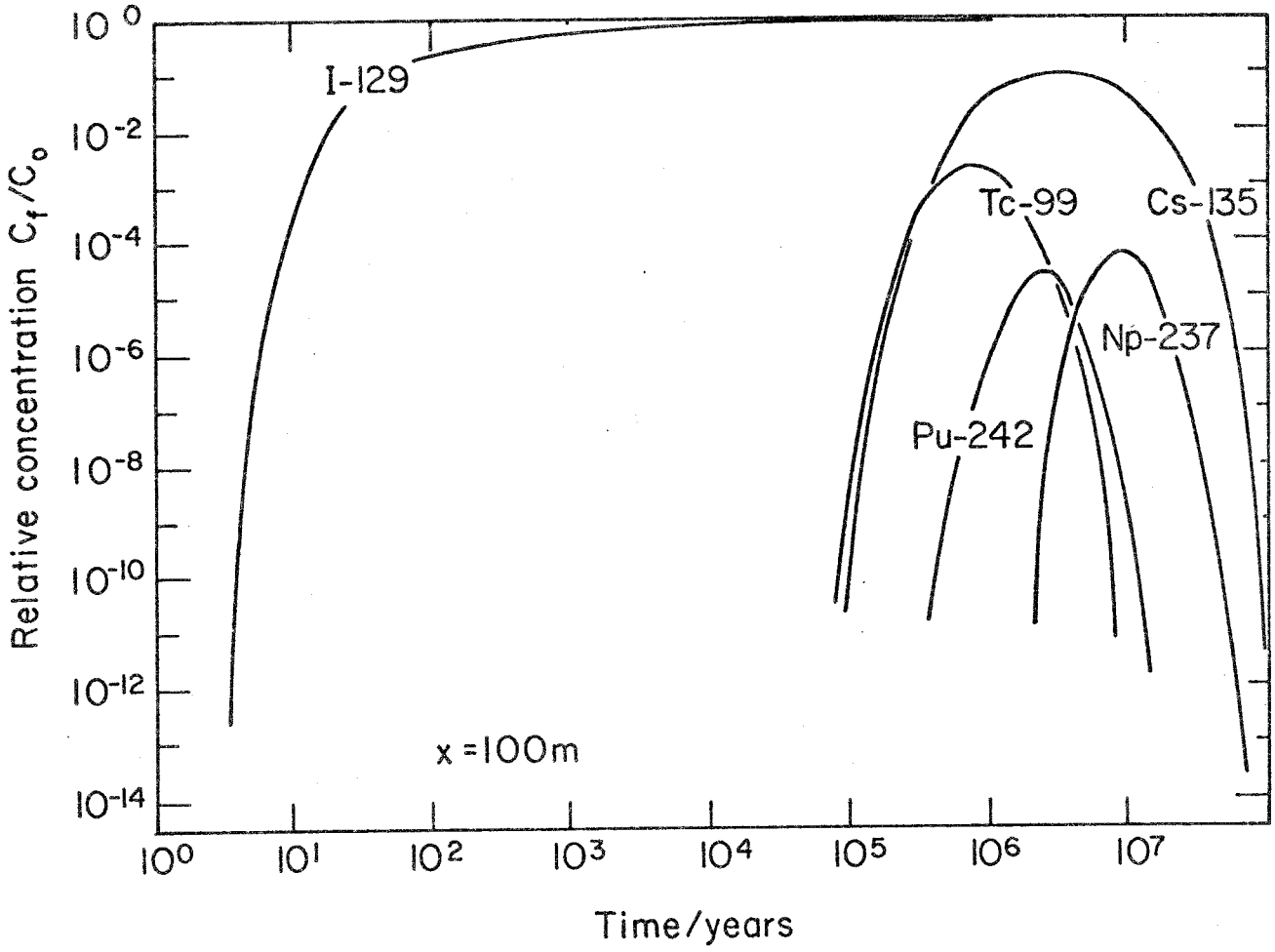
Relative concentration C_f/C_o
10^0
10^{-2}
10^{-4}
10^{-6}
10^{-8}
10^{-10}
10^{-12}
10^{-14}
I-129
Tc-99
Cs-135
Np-237
Pu-242
x = 100m
10^0
10^1
10^2
10^3
10^4
10^5
10^6
10^7
Time/years

FIGURE 14

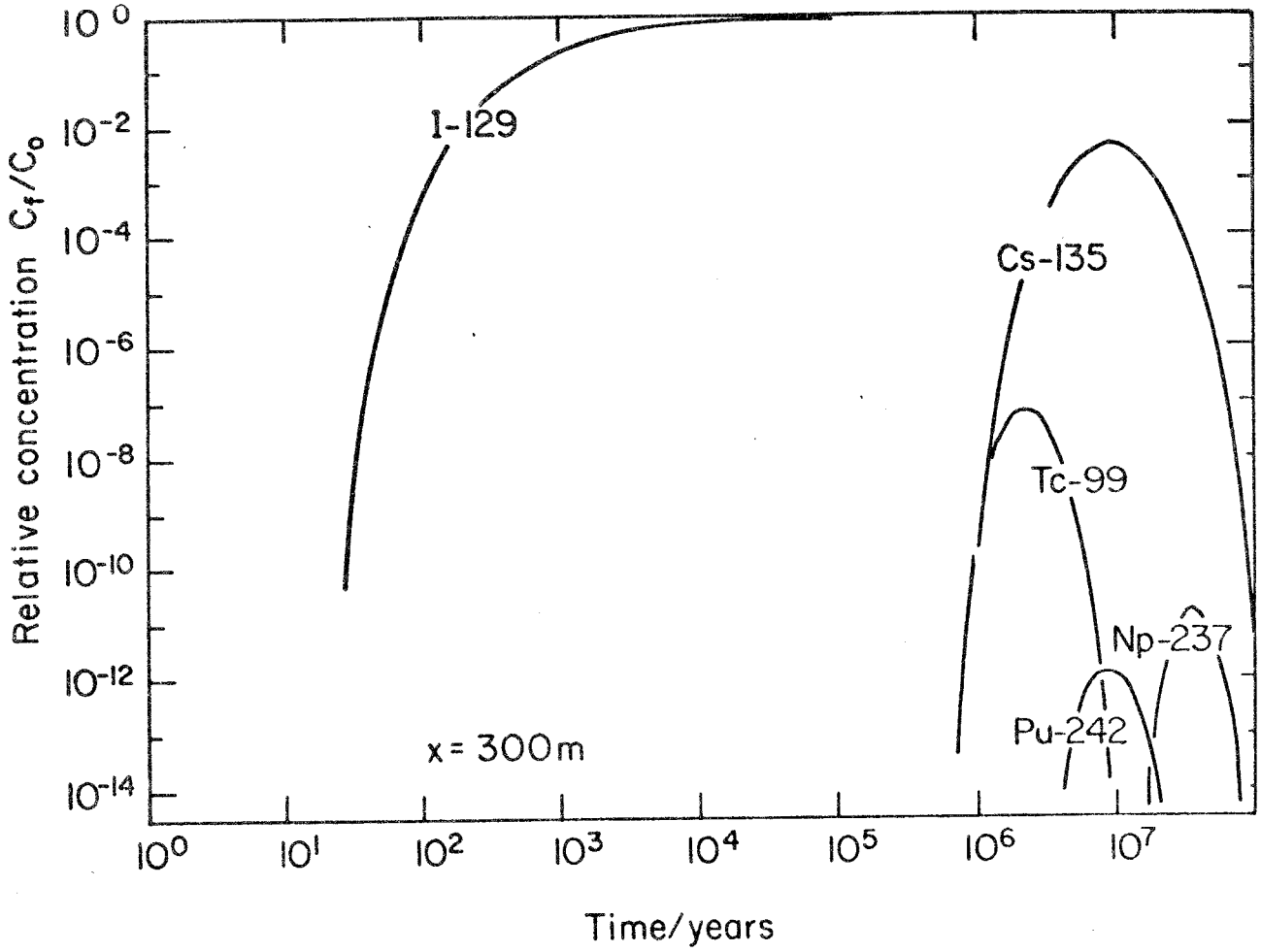
Relative concentration C_f/C_o
10^0
10^{-2}
10^{-4}
10^{-6}
10^{-8}
10^{-10}
10^{-12}
10^{-14}
I-129
Cs-135
Tc-99
Np-237
Pu-242
x = 300m
10^0
10^1
10^2
10^3
10^4
10^5
10^6
10^7
Time/years

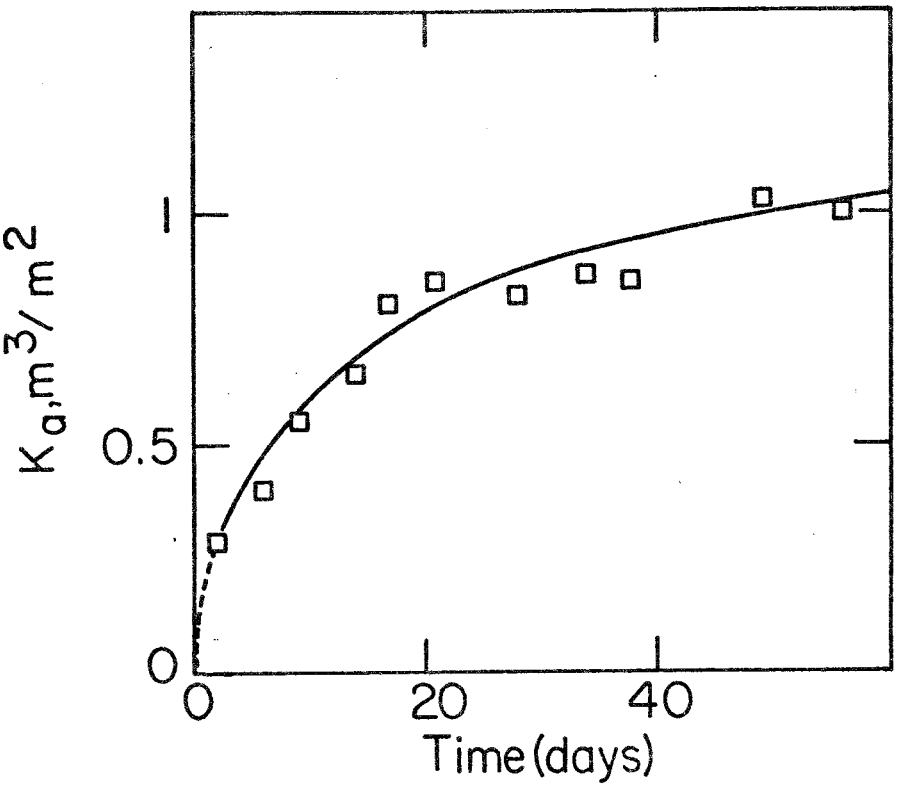

Figure 15 Sorption of cesium on carbonate rock (Rancon, 1967).

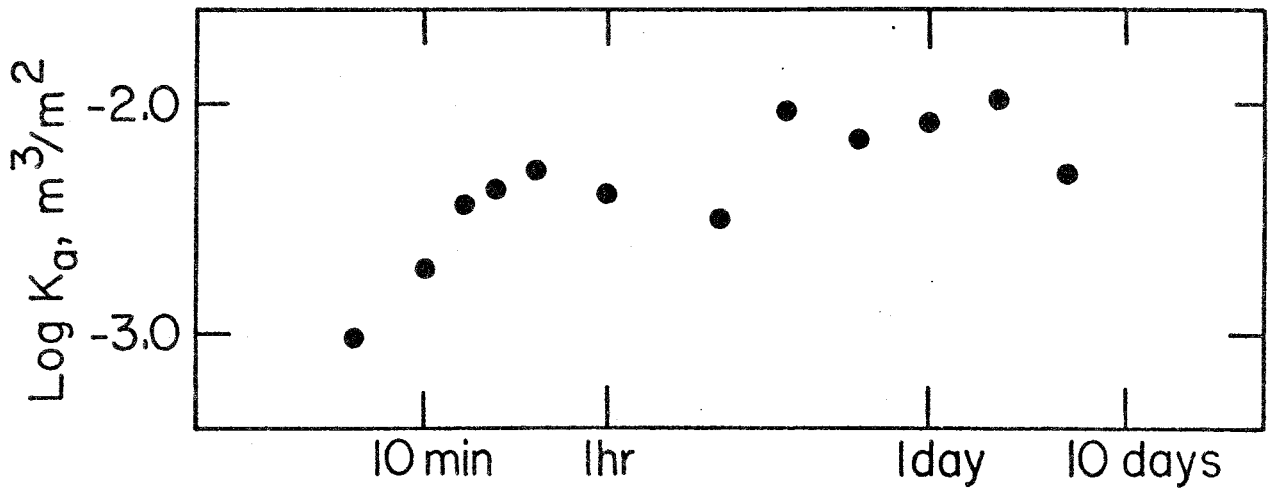

Figure 16 Sorption of strontium on a granite surface (Allard, 1978).

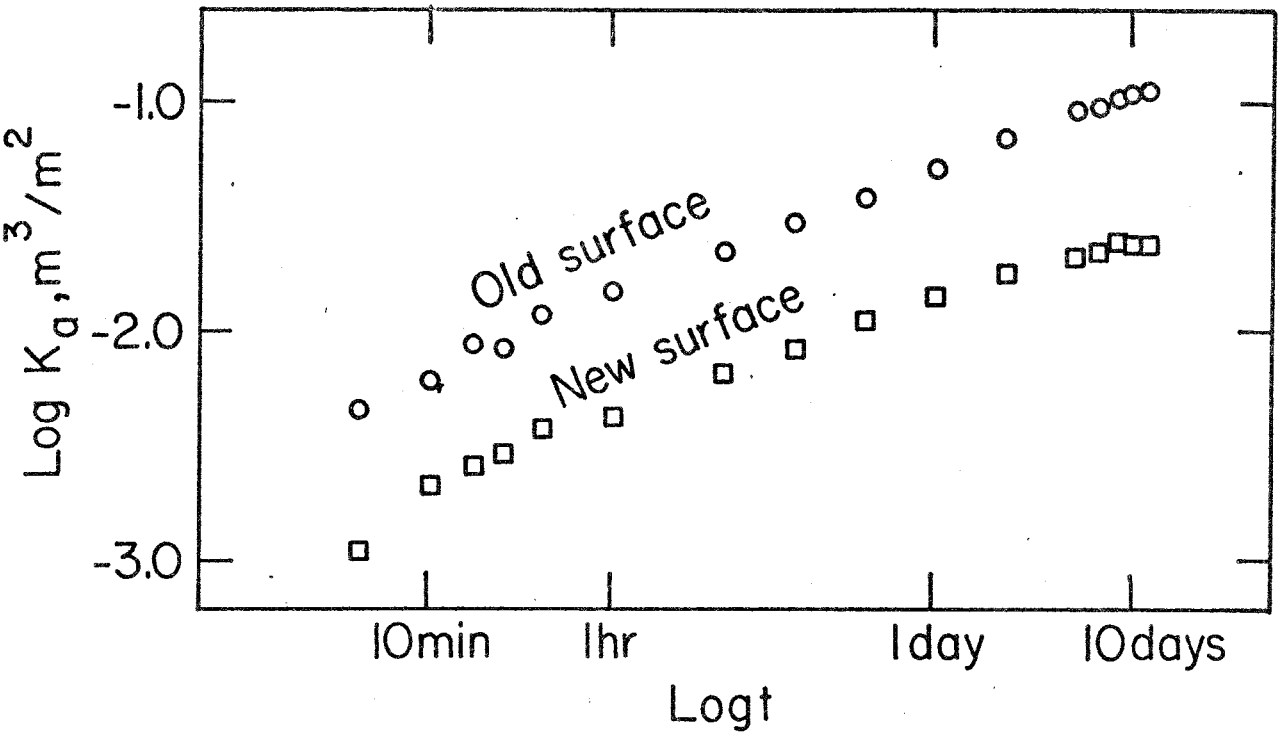

Figure 17 Sorption of cesium on granite surface (Allard, 1978)

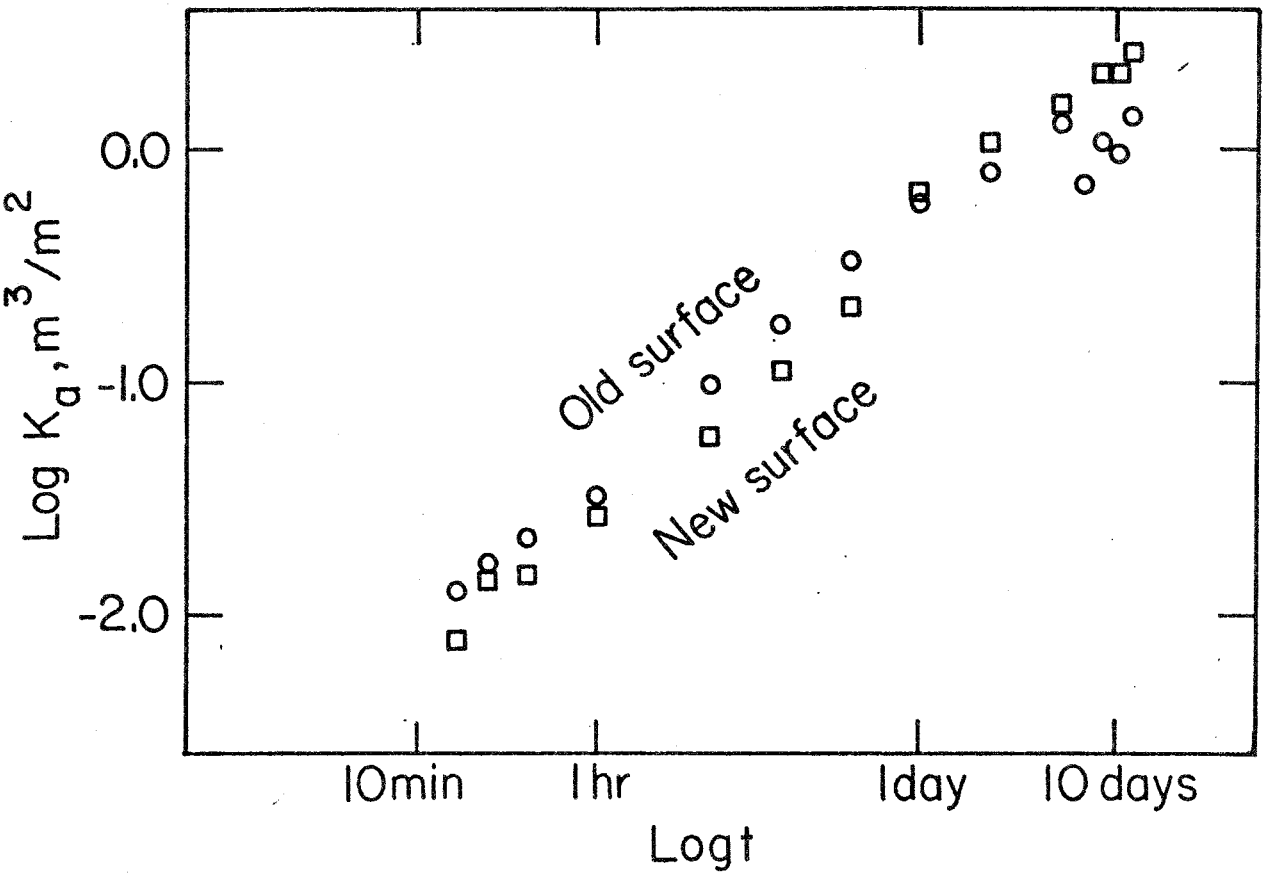

Figure 18 Sorption of americium on granite surface (Allard, 1978).

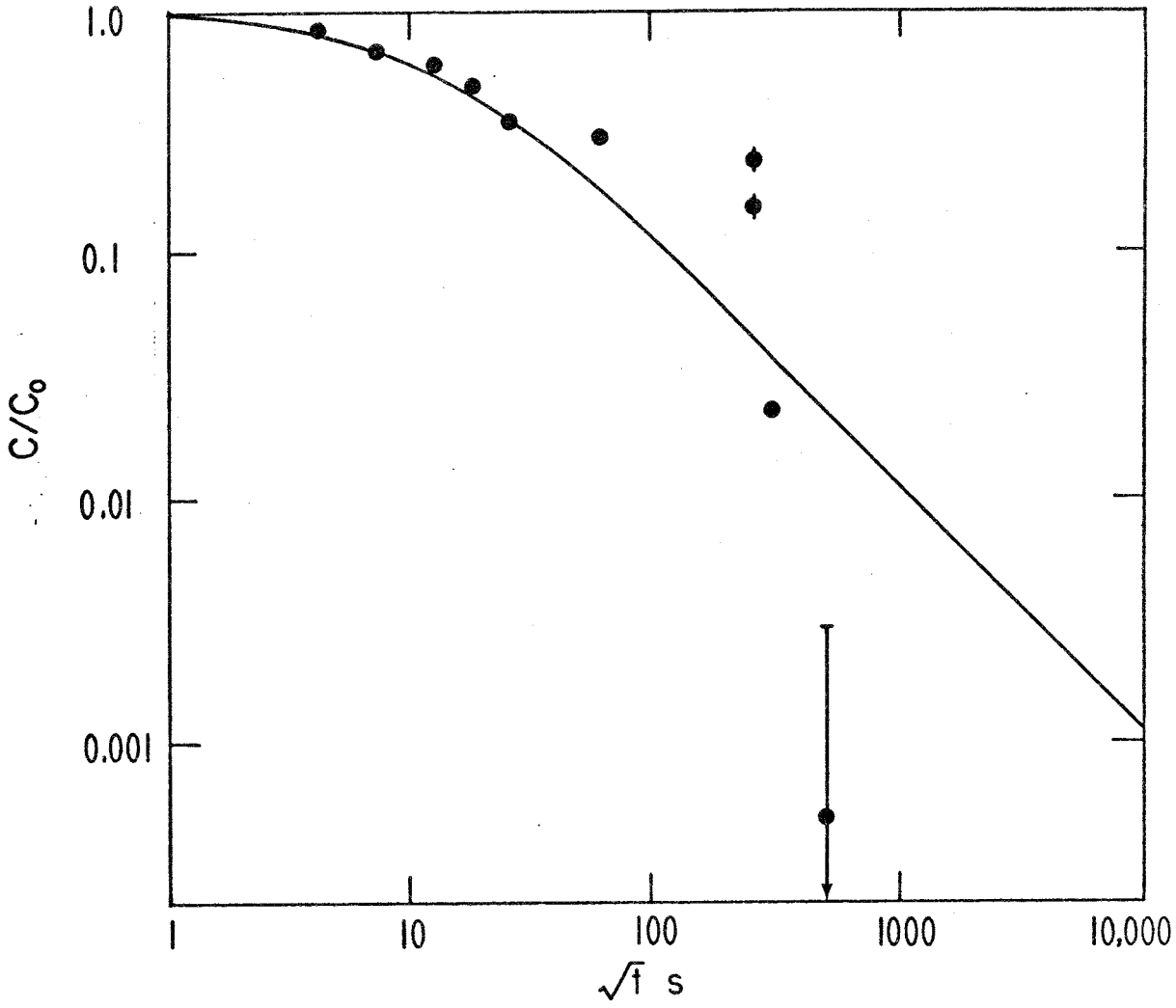

Figure 19 Sorption of americium on granite surface (Seitz, 1978).

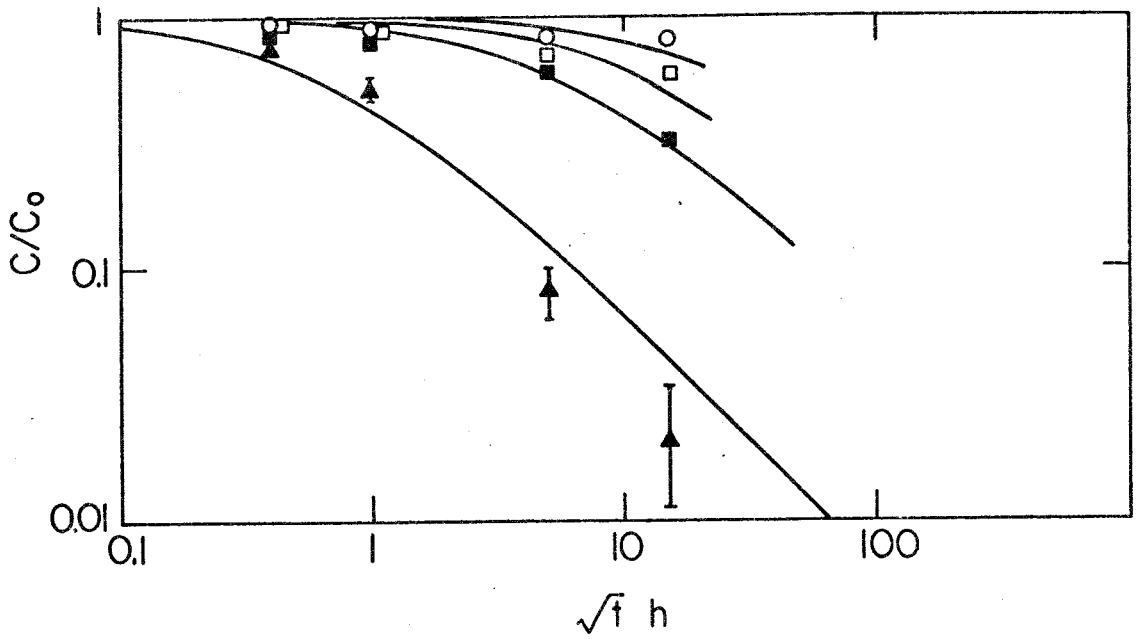

Figure 20 Sorption of Cs, Sr and Am on old and new granite surfaces (Allard, 1978).

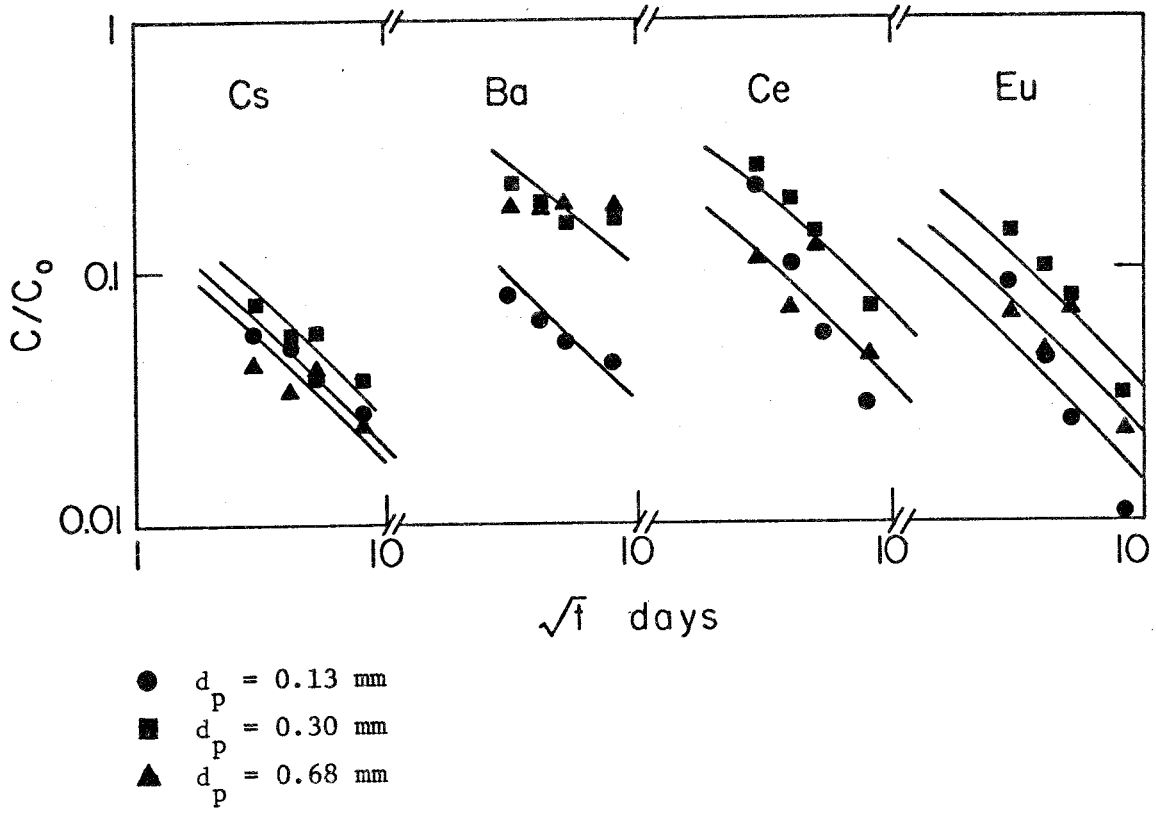

Figure 21 Sorption of radionuclides on granite particles. Ambient temperature (Erdal, 1978).

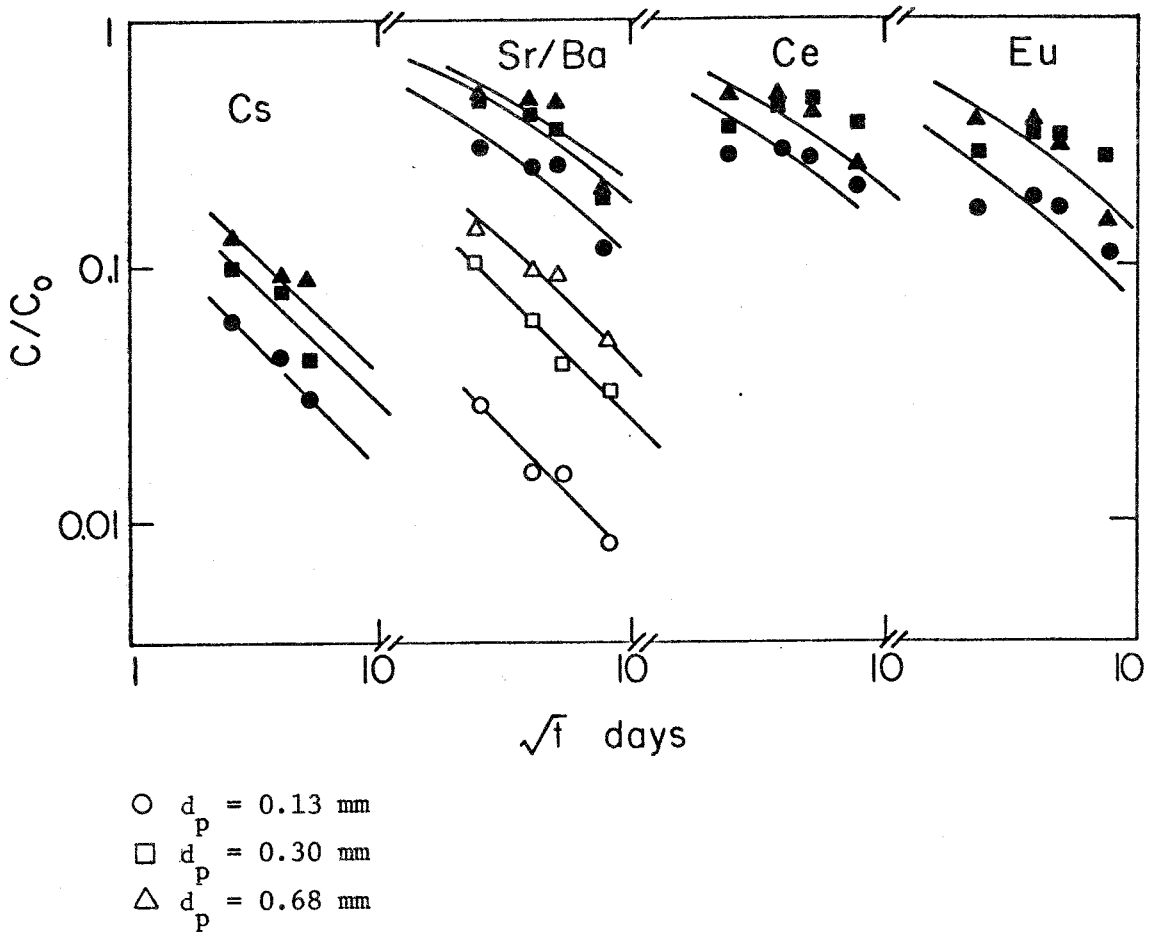

Figure 22 Sorption of radionuclides on granite particles 70°C (Erdal, 1978).

FÖRTECKNING ÖVER SKBF PROJEKT KBS TEKNISKA RAPPORTER

79-01 Clay particle redistribution and piping phenomena in bentonite/ quartz buffer material due to high hydraulic gradients
Roland Pusch
University of Luleå 1979-01-10

79-02 Försöksområdet vid Finnsjön
Beskrivning till berggrunds- och jordartskartor
Karl-Erik Almén
Lennart Ekman
Andrzej Olkiewicz
Sveriges Geologiska Undersökning november 1978

79-03 Bergmekanisk bedömning av temperaturbelastning vid slutförvaring av radioaktivt avfall i berg
Ove Stephansson
Bengt Leijon
Högskolan i Luleå 1979-01-10

79-04 Temperatur- och spänningsberäkning för slutförvar
Taivo Tarandi
VBB Vattenbyggnadsbyrån, Stockholm februari 1979

79-05 Kompletterande berggrundsundersökningar inom Finnsjö- och Karlshamnsområdena
Andrzej Olkiewicz
Sören Scherman
Karl-Axel Kornfält
Sveriges Geologiska Undersökning 1979-02-02

79-06 Kompletterande permeabilitetsmätningar i Karlshamnsområdet
Gunnar Gidlund
Kenth Hansson
Ulf Thoregren
Sveriges Geologiska Undersökning februari 1979

79-07 Kemi hos berggrundvatten i Blekinge
Gunnar Jacks
Institutionen för Kulturteknik, KTH, februari 1979

79-08 Beräkningar av grundvattenrörelser inom Sternöområdet i Blekinge
John Stokes
Institutionen för Kulturteknik, KTH, februari 1979

79-09 Utvärdering av de hydrogeologiska och berggrundsgeologiska förhållandena på Sternö
Kaj Ahlbom
Leif Carlsson
Gunnar Gidlund
C-E Klockars
Sören Scherman
Ulf Thoregren
Sveriges Geologiska Undersökning, Berggrundsbyrån, februari 1979

79-10 Model calculations of groundwater condition on Sternö peninsula
Carl-Lennart Axelsson
Leif Carlsson
Geological Survey of Sweden september 1979

79-11 Tolkning av permeabilitet i en befintlig berganläggning
Ulf Lindblom
Alf Norlén
Jesús Granero
Kent Adolfsson
Hagconsult AB februari 1979

79-12 Geofysisk borrhålsmätning i 2 st borrhål på Sternö
Kurt-Åke Magnusson
Oscar Duran
Sveriges Geologiska Undersökning februari 1979

79-13 Bildning av fritt väte vid radiolys i lerbädd
Trygve Eriksen
Johan Lind
Institutet för Kärnkemi KTH 1979-03-28

79-14 Korrosionsprovning av olegerat titan i simulerade deponeringsmiljöer för upparbetat kärnbränsleavfall. Slutrapport.
Sture Henrikson
Marian de Pourbaix
Studsvik Energiteknik AB 1979-05-07

79-15 Kostnader för hantering och slutförvaring av högaktivt avfall och använt kärnbränsle
Arne W Finné
Åke Larson Byggare, april 1979

79-16 Beräkning av permeabilitet i stor skala vid bergrum i Karlshamns hamn
Ulf Lindblom
J J Granero
Hagconsult AB Göteborg, 23 augusti 1979

79-17 Water percolation effects on clay-poor bentonite/quartz buffer material at high hydraulic gradients
R Pusch
Div. Soil Mechanics, University of Luleå, 1979-05-31

79-09 Utvärdering av de hydrogeologiska och berggrundsgeologiska förhållandena på Sternö
Kaj Ahlbom
Leif Carlsson
Gunnar Gidlund
C-E Klockars
Sören Scherman
Ulf Thoregren
Sveriges Geologiska Undersökning, Berggrundsbyrån, februari 1979

79-10 Model calculations of groundwater condition on Sternö peninsula
Carl-Lennart Axelsson
Leif Carlsson
Geological Survey of Sweden september 1979

79-11 Tolkning av permeabilitet i en befintlig berganläggning
Ulf Lindblom
Alf Norlén
Jesús Granero
Kent Adolfsson
Hagconsult AB februari 1979

79-12 Geofysisk borrhålsmätning i 2 st borrhål på Sternö
Kurt-Åke Magnusson
Oscar Duran
Sveriges Geologiska Undersökning februari 1979

79-13 Bildning av fritt väte vid radiolys i lerbädd
Trygve Eriksen
Johan Lind
Institutet för Kärnkemi KTH 1979-03-28

79-14 Korrosionsprovning av olegerat titan i simulerade deponeringsmiljöer för upparbetat kärnbränsleavfall. Slutrapport.
Sture Henrikson
Marian de Pourbaix
Studsvik Energiteknik AB 1979-05-07

79-15 Kostnader för hantering och slutförvaring av högaktivt avfall och använt kärnbränsle
Arne W Finnē
Åke Larson Byggare, april 1979

79-16 Beräkning av permeabilitet i stor skala vid bergrum i Karlshamns hamn
Ulf Lindblom
J J Granero
Hagconsult AB Göteborg, 23 augusti 1979

79-17 Water percolation effects on clay-poor bentonite/quartz buffer material at high hydraulic gradients
R Pusch
Div. Soil Mechanics, University of Luleå, 1979-05-31

79-18 Sammanställning och utvärdering av genomförda GETOUT- och BIOPATH-körningar
M Elert
B Grundfelt
C Stenquist
Kemakta AB, Studsvik Energiteknik AB, 1979-08-13

79-19 Diffusion in the rock matrix - An important factor in radionuclide retardation?
Ivars Neretnieks
Royal Institute of Technology May 1979

79-20 Hydraulisk konduktivitet bestämd i stor skala i ytliga partier av Blekinge kustgnejs
Ulf Lindblom, Hagconsult AB, Göteborg
Torbjörn Hahn, Fortifikationsförvaltningen, Stockholm
Göteborg juni 1979